Development of SPT inhibitor for treatment of Hereditary Sensory Autonomic Neuropathy and Macular Telangiectasia

Responsible:
Professor Auwerx Johan

Supervisors:
Bachmann Alexis, Romani Mario

Authors:
Bender Audrey, Claudet Marion, Dratva Lisa,
Lasne Charlotte, Margaria Juliette, Melis Jonathan,
Morandini Francesco, Seddiki Anas, Vinzant Hugues,
von Alvensleben Giacomo

EPFL

Scientific project design in drug discovery – 2019

Table of Contents

Abstract

Hereditary sensory neuropathy (HSN) and Macular Telangiectasia (MacTel) are two orphan diseases characterized by an accumulation of atypical sphingolipids exhibiting significant neurotoxicity. In HSN, the peripheral sensory neurons are impaired, whereas in MacTel photoreceptor cells are affected, and to date no treatment exists for either pathology. In both conditions toxic lipid molecules are synthesized by the enzyme Serine Palmitoyl-Transferase (SPT), which is a membrane-bound dimer made up of two distinct subunits that are ubiquitously expressed. SPT synthesizes the first step of *de novo* synthesis of ceramide, an important sphingolipid whose dysregulation is implicated in various molecular processes and a wide range of diseases.

We propose to develop a new oral drug which inhibits toxic ceramide synthesis by disrupting the formation of the *SPTLC1/SPTLC2* dimer. As no treatment is available to prevent further progression for either pathologies, they constitute relevant targets to improve life quality of affected patient. Both conditions have a great impact on daily life; photoreceptor atrophy in MacTel condition can lead to loss of central vision; whereas paralysis, loss of sensory and stabbing pain represent symptoms of HSN. An oral route of administration is chosen to facilitate patient long-term treatment.

We present a complete pipeline comprising all stages of the industrial drug discovery process up to market access, resulting in a novel drug treatment for both HSN and MacTel. After an extensive virtual screen discriminating for the best physical properties, a series of primary in vitro tests is performed. Optimization of structure and mechanism ensues together with toxicity testing in cells. Molecules exhibiting successful structure-activity relationships will be further tested in mouse models to determine the pharmacodynamics and in vivo toxicity of the candidates and evaluate the optimal dosage of the selected drug. Along the in-vitro and in-vivo phases, the pool of candidate drugs is continuously reduced trough an iterative and refinement process, ending up with a final molecule. The optimal dosage will then be validated in clinical trials, where the effect on the disease is studied in patients. Successful clinical trials will pave the way for market access of our drug.

The unmet medical need and severe consequences of both diseases are key for an accelerated submission process to receive a patent earlier and reduce development cost. Furthermore, patent protection extension for orphan disease drugs will shield our drug from competition, allowing higher return of investment and more time to explore new opportunities of treatment.

Introduction

With our proposal we address the urgent need of individuals suffering from accumulation of toxic lipid molecules as a result of abnormal enzymatic activity of Serine Palmitoyl-Transferase (SPT). SPT catalyzes the first and rate-limiting step of the *de novo* synthesis of ceramide.

Ceramides

Ceramides are lipophilic molecules composed of a spingoid base linked to a fatty acid. They are pivotal in sphingolipid biosynthesis and breakdown, as all main sphingolipid pathways converge and stem from ceramide[1]. Figure 1 depicts the *de novo* pathway of ceramide synthesis, with SPT clearly positioned in the membrane of the Endoplasmic Reticulum (ER). See also Table 4 from the supplementary information for a list of all enzymes involved. Ceramides make up a significant fraction of lipids in the eukaryotic cell membrane and were originally thought to be only of structural support to cells. Recent research however has uncovered the regulatory functions of ceramide in many important processes in the human body: signaling for cell proliferation and programmed cell death, inflammation, nervous signal transduction, angiogenesis, and more[2]. Ceramide dysregulation has been linked to the development of a wide range of pathologies, including neurodegenerative diseases like Alzheimer's and Parkinson's[3], different types of cancer, obesity, diabetes and genetic disorders such as Gaucher's disease[4]. Depending on the disease and the symptoms observed, accumulation or deprivation of ceramide levels are associated with the severity of the pathological condition, complicating the search for causal relationships in those diseases.

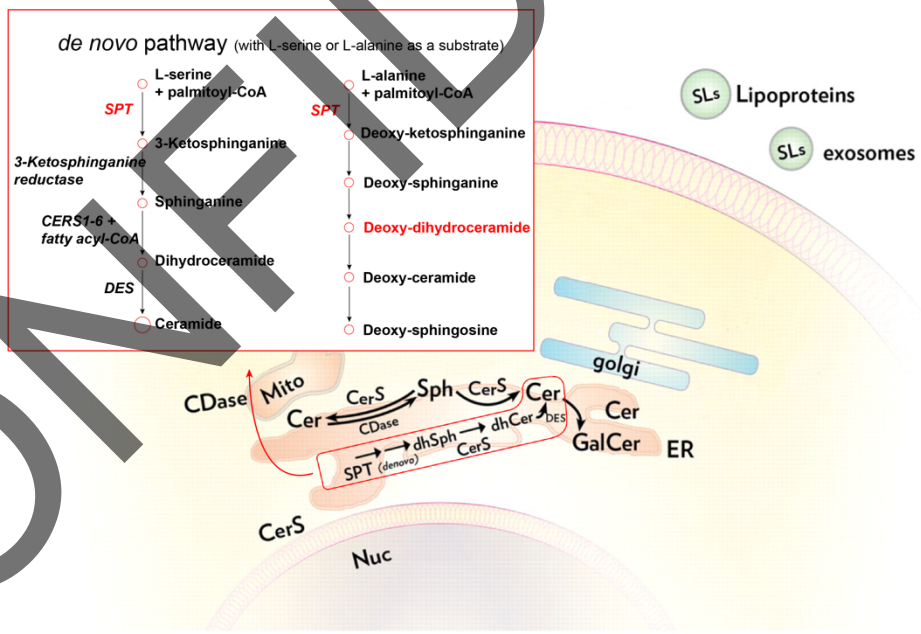

Figure 1 - de novo pathway of ceramide synthesis

We have identified our target enzyme after extensive analysis of all proteins involved in the ceramide pathway whereby we compared their expression in different tissues, cellular location, previously reported experimental

results, availability of 3D structures, and phenotypes for known variants or mutations. A list of our investigated targets can be found in the supplementary information in form of a table, together with information currently available for the proteins. We investigated different intermediates such as the ones participating in the sphingolipid rheostat, where Niemann-Pick disease would have been another candidate pathology without an existing treatment[5]. However, since most protein structures are not resolved, we exclude them as targets. Other enzymes considered were the sphingosine kinases and lyases, but no diseases resulted directly from mutations in those genes. We conclude that targeting the enzyme SPT has the biggest potential impact for patients while minimizing our chances of failure.

Target diseases

In this report we will focus on two different pathologies characterized by the same observed toxicity in neuronal cells. As they share molecular similarities, we have devised our drug discovery process around the common elements of the diseases to allow a treatment for both conditions with a common pipeline.

Hereditary sensory neuropathy Type 1 (HSN1) is a progressive neurological disorder characterized by distal sensory loss inducing tingling, weakness and reduced ability to feel pain and temperature[6]. This neuropathy is thought to be a hereditary disorder due to the higher frequency of the disease occurrence observed in families with a confirmed HSN1 affected individual. The exact prevalence of the disease remains unknown due to frequent misdiagnosis but is estimated in a range from 2/100'000[7] to 2/1'000'000[8]. The onset of symptoms in affected individuals can lie anywhere between 20 and 50 years of age, and at advanced stages the disease can lead to chronic skin ulcers and even require distal amputation. Although HSN1 is neither life-threatening nor life-shortening, patients' quality of life is heavily impaired, making early diagnosis and appropriate treatment crucial. HSN is the collective term for four different types of the condition, all characterized by the loss of sensibility and autonomic dysfunction. Type 1 is the most studied and prevalent, whereas Type 2 and Type 4 have very low prevalence worldwide and Type 3 is almost exclusively observed in individuals of eastern European Jewish descent. The exact frequencies are not known[9,10].

In HSN1, a mutation in the *SPTLC1* gene causes a substrate preference shift of the enzyme from L-serine to L-alanine. The most common mutation of this type is $SPTLC1^{C133W}$ [11], a change from cysteine to tryptophan in position 133 of *SPTLC1*. This leads to the formation of an atypical class of deoxysphingolipids. Their changed molecular structure cannot be effectively degraded in the cell leading to an accumulation in the plasma that is toxic to neurons. The pathogenicity is characterized by cytoskeletal changes and disassembly of actin stress fibers. Moreover, *SPTLC1* expression is ubiquitous in the body and not tissue specific.

Macular telangiectasia (MacTel) is an ophthalmic pathology of the macula leading to abnormalities in the capillaries of the fovea and to neurosensory atrophy. MacTel Type 2 is acquired and bilateral, and usually manifests in subjects between 50 and 70 years of age. This is the most common form of the disease. The recently evaluated prevalence lies in between 45/1'000'000 and 6/10'000[12]. According to the MacTel Project, half of all Type 2 patients show a loss of up to 50% of their visual acuity[13] [14]. The causes of the disease still need to be established but studies have shown a link to a mutation located on the *SPTLC2* gene[Erreur ! Signet non défini.]. This could explain the accumulation of toxic deoxysphingolipids that lead to Müller cell degeneration, subsequent neuronal loss, depigmentation and progressive central macular thinning. Other studies in patients without any mutation on the *SPTLC1* or *SPTLC2* gene have shown MacTel to also be associated with low serine levels in blood. At low serine levels, a shift in the substrate of SPT from L-serine to L-alanine was present even without the mutation. Insufficient blood serine levels are thus a possible cause for the disease in patients without mutation that show symptoms of MacTel.

The determination of the causes of MacTel is challenging due to its incomplete penetrance and its complex inheritance patterns. As a multifactorial condition, it can be caused by mutations in *SPTLC1* or *SPTLC2*. *Gantner and al*. have shown that the disease can also be observed when the same molecular mechanism underlying certain cases of HSN1 is present.

Drug discovery process overview

In this report we will primarily propose a drug development process for the treatment of HSN1 and MacTel Type 2. A first phase of virtual screening allowing to identify a library of candidate compounds will be followed by an extensive *in vitro* experimentation step. During this process, the number of compounds will be reduced, and the best candidates will then be tested *in vivo* on mouse models. Our hit-to-lead choice will allow production of a new drug whose efficiency will be demonstrated in the abovementioned rare mendelian pathologies to take advantage of facilitated and sped up approval procedures for orphan diseases. We will also benefit from a 2-year extension on our patents in that case. Because of the common mechanism of the above described diseases, which leads to an accumulation of toxic deoxysphingolipids, a common drug can be developed treating both pathologic conditions. In the final section of this proposal, clinical trials are described for phases 1 to 4. The complete pipeline is depicted in form of a flow chart in Figure 2.

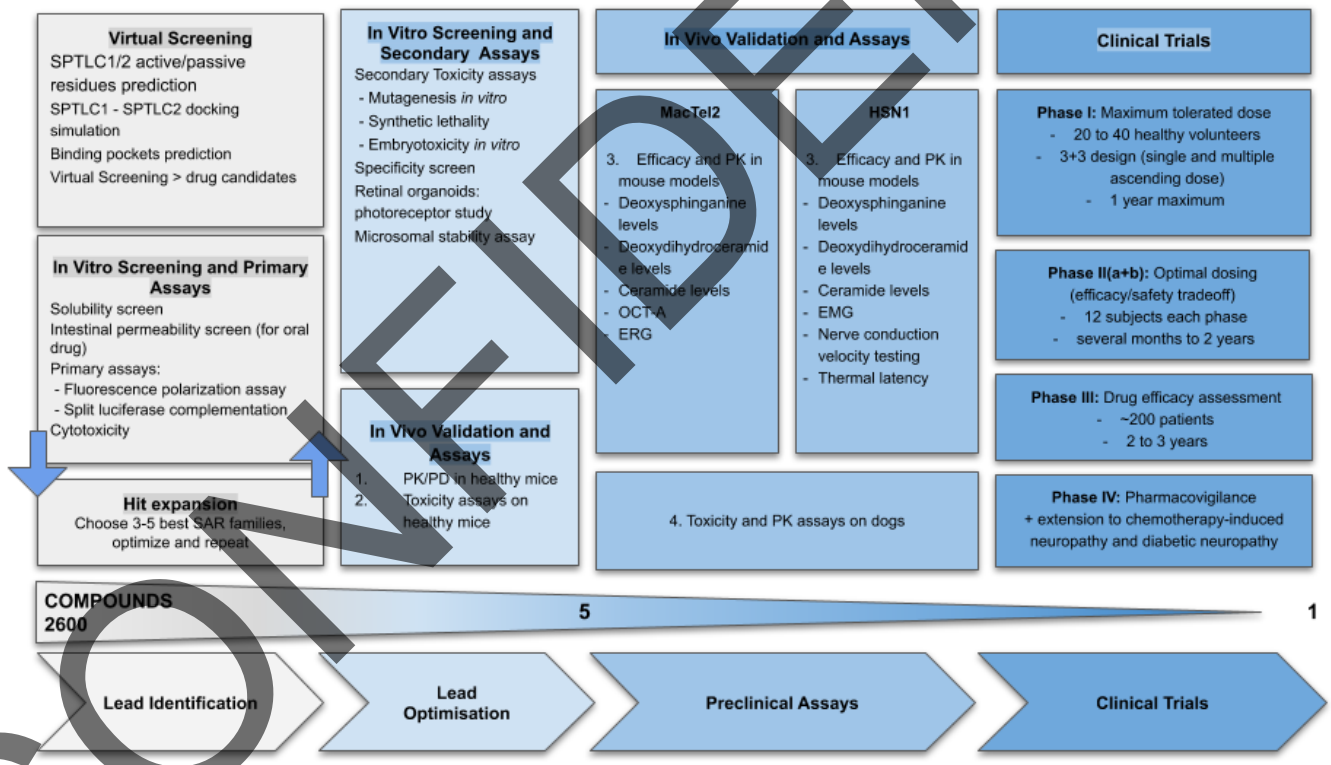

Figure 2 - Flow chart summarizing the drug discovery process

After gaining market approval, our emerging company will expand its R&D efforts to treat more common conditions. A growing body of evidence shows that our targeting strategy can be extended to treat certain chemotherapy-induced neuropathies (namely paclitaxel)[85] as well as diabetic peripheral neuropathies[88]. Indeed, the production of toxic sphingolipids by SPT are involved in both conditions and were found to be correlated with decreased L-serine levels. Thus, we hypothesize that our final drug candidate will reduce the

cancer treatment side-effects enabling an appropriate paclitaxel dose administration and might be used as a novel therapeutic approach in the case of diabetic neuropathy.

Virtual screening

To identify drug candidates, virtual screening is the first technique adopted by our company. The targeted drug is an inhibitor of SPT heterodimerization from *SPTLC1* and *SPTLC2* or *SPTLC3* homodimers. *SPTLC3* presents 63% homology with *SPTLC2* and its expression is highly variable in different tissues[15]. Only *SPTLC1* and *SPTLC2* are however considered in this study because of their complete characterization and predominance. The interactions between those proteic subunits are also confirmed by a *STRING*[16] protein-protein network analysis (Figure 10 and Table 1). Of particular importance is the fact that ORMDL3 is also present in the network. ORMDLs are a set of highly conserved proteins bound to the ER that form stable complexes with SPT[17]. Depending on the level of sphingolipids, this interaction has an inhibitory or non-inhibitory character for high and low sphingolipids concentrations respectively. The same effect is observed when the mutant SPT^{C133W} is present[18]. In particular, ceramides are suggested as the sphingolipids causing this switch. The targeted mode of action of our drug is independent of this inhibition mechanism. Moreover, since the level of ceramides might be affected in our disease, exploiting ORMDL3 inhibition could not be effective.

Human structures for both *SPTLC1* and *SPTLC2* exist and can be accessed in the SWISS-MODEL database[19]. Those structures are homology models based on the *S. paucimobilis* bacterial SPT structure (pdb code 4bmk.1.A), which is constructed by x-ray diffraction with a resolution of 1.62Å. Model A and B of the subunits exist and have a very high degree of similarity between them; for all the virtual screening analyses, model A is selected.

Then, an in-depth structural analysis of the enzyme subunits is performed. Since no assembling documentation exists for the human SPT, a docking analysis between *SPTLC1* and *SPTLC2* is carried out with *HADDOCK 2.4* software[20] to identify the dimer's interface. Active and passive protein-protein surface residues (Figure 12) are predicted with the experimental data-driven *CPORT* algorithm[21] and used as inputs for *HADDOCK 2.4*. The same simulations are repeated also for the most common *SPTLC1* mutation, $SPTLC1^{C133W}$, keeping the $SPTLC2^{WT}$. With the docking simulation results the polar contact sites, defined here as residues involved in H-bonds, are determined (Figure 3 A, B). Docking with *SPTLC2* considerably differs for $SPTLC1^{WT}$ and $SPTLC1^{C133W}$ (Figure 13) but interestingly *SPTLC2* always docks approximately on the same region of *SPTLC1*. It is important to notice that the C133W residue is involved in the polar binding for $SPTLC1^{WT}$ but not for the $SPTLC1^{C133W}$ mutant (Figure 3C and Table 2). This could explain the change in substrate affinity when the mutation is present.

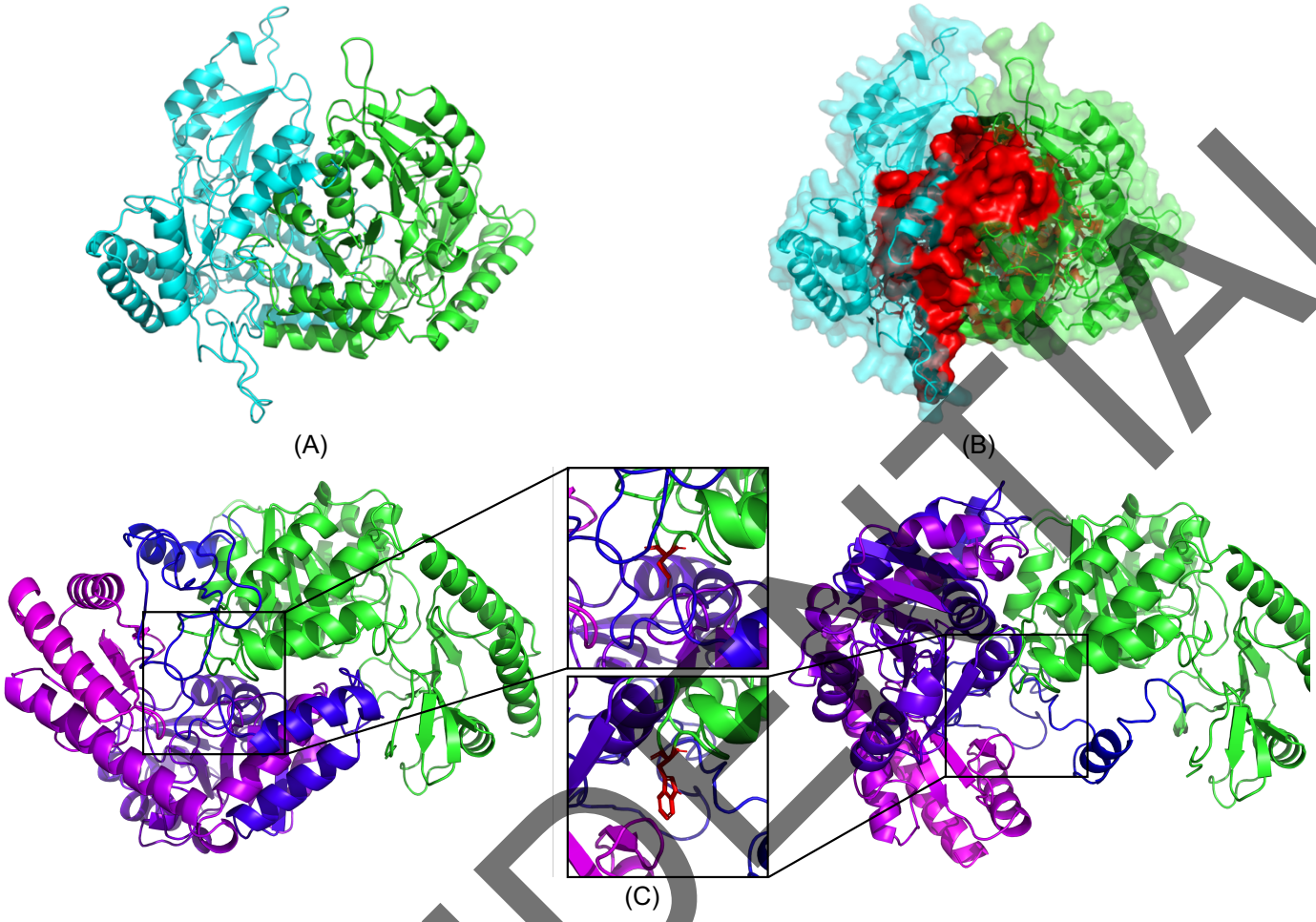

Figure 3 - HADDOCK docking predictions visualizations for SPTLC1 and SPTLC2 interaction. Figures are generated with PyMOL. (A) Haddock protein-protein docking interaction visualization. Green: SPLTC1; Blue: SPTLC2. (B) Interface area (red) computed with InterfaceResidues PyMOL script. (C) Visualization of the 133C (top box) and 133W (bottom box) residues in SPTLC1^{WT} (left) and SPTLC1^{C133W} (right) respectively.

An analysis to identify the potential binding sites for small molecules on the enzymes surfaces is performed with *GHECOM 1.0* algorithm[22], using a maximum radius for the large probe (pocket shallowness) of 10 Å. This tool uses mathematical morphology to predict surface pockets; results are reported in Figure 11. The analysis is qualitative and only gives a rough idea of which target sites and the corresponding targeting molecular candidates could be the most appropriate and effective. However, because of its simplicity results can be considered as additional selection criteria for which molecules identified in the next section should receive particular attention for *in vitro* testing.

Virtual screening is run for some of the identified polar-contact residues. The adopted screening strategy makes use of the *LEA3D*[23] software applied on those binding targets. This tool allows to generate a set of candidate molecules from existing drug fragments combination by maximizing a docking score and some molecular properties like the Lipinski's Rule of Five[24]. The advantage of this approach is indeed the multi-factors fitness score, considering the ADME properties and the docking likeliness. In addition, the bottom-up generation approach described later allows a reduced computational cost. The detailed procedure explaining the residue selection criteria and the screening algorithm is detailed in the supplementary information. A total of 51x8 = 408 candidate molecules targeting 8 different regions of the SPT dimer contact region are generated. By application of a threshold on the final overall LEA3D score, a library can be selected. For

example, by applying a 92% threshold, 130 candidates are initially considered. Only the 8 best candidate for each binding site are shown in **Erreur ! Source du renvoi introuvable.** among the total of 130 selected molecules.

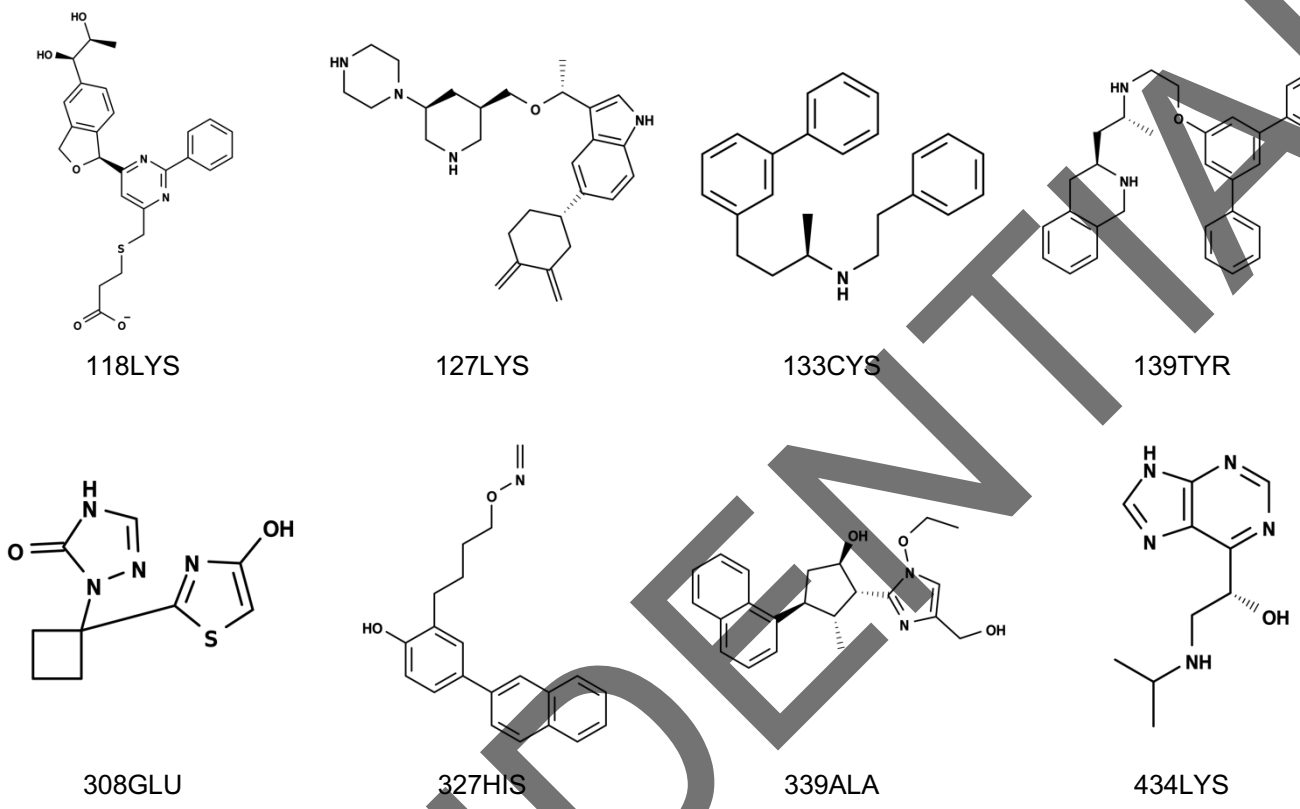

Figure 4 - Best candidate for each targeted binding site and fitness score constructed by the LEA3D genetic algorithm. The name indicates the SPTLC1^{WT} residue used as central binding site in LEA3D simulations. In total, 130 molecules are selected in our library.

To expand the built library before the next *in vitro* tests, functional groups can be added *in silico* to the compounds[25]. This approach allows to introduce greater variability of the explored chemical space, always maintaining a drug-like library potentially targeting the *SPTLC1-SPTLC2* dimerization interface because of chemical similarity. This procedure is usually performed by specialized chemists that can take advantage of software helping with the mapping and the visualization of the functional groups on a candidate molecule[26]. An example of software is *SILCS*, exploiting molecular dynamics simulations combined with experimental data to provide a map of binding sites of small molecular fragments such as functional groups[27]. Modifications of the molecules can be designed and tested with this approach. In this expansion process, the ability and the creativity of the chemist are essential to guarantee that the designed compounds are easily synthesizable. However, to overcome this last problem, recently some deep-learning algorithms predicting the feasibility and steps of a chemical synthesis have been developed[28]. Those tools, together with some fragment-based approaches similar to the one described for the LEA3D algorithm, could be used to virtually expand the library for the next phases. From the experience of a chemist of the EPFL Biomolecular Screening Facility (BSF)[29], a 20-fold expansion could for example be considered, leading the number of candidates in our libraries to 2600.

Prior to *in vitro* analysis, some analogous tests can be performed *in silico*. A toxicology test can be for example executed using the free OpenVirtualToxicLab software[30]. By running docking simulations with the molecules in the libraries, potential toxicity can be assessed, allowing to exclude some candidates from further experimental tests. A list of 16 proteins known to trigger side-effects is used as target, covering some carcinogenicity and cardiotoxicity effects as well as some metabolic and endocrine disruptions. Among those proteins, nuclear receptors, transmembrane channels, transcription factors and some cytochrome entities are present.

Other basic interesting virtual analysis overlapping with the next steps of the drug development could be performed with existing tools. For example, predictions for pharmacokinetics properties[31] or biodegradation pathways[32] could be considered. Quantitative structure-activity relationships (QSAR) machine-learning analyses exploiting one of the several existing software[33] could also be interesting.

To test our final library of candidates *in vitro*, the chemical structures are submitted to an external company for custom synthesis. Merck[34] or KareBay Biochem[35] are good examples of cooperating partners.

Validation of the Mode of Action

To validate the possible therapeutic effect of our drug, we first have to show that our chosen mode of action will indeed lead to reduced levels of sphingolipids in cells. We need an experiment that investigates the effect of inhibition of dimer formation on sphingolipid and ceramide levels overall.

Studies have shown[36] that *SPTLC1*(-/-) mice are embryonic lethal, as are *SPTLC2*(-/-) mice, meaning that both units have to be present during development. However, it is not certain that simply inhibiting dimerization of *SPTLC1* and *SPTLC2* would inhibit enzymatic activity significantly. We could investigate this issue by engineering a modified gene sequence for *SPTLC1* or *SPTLC2* such that a large amino acid side chain will appear in the middle of the dimer binding site. The point sense mutations will be introduced for the interaction residues identified with virtual screening. We hypothesize that this side chain will prevent dimerization of the two subunits (which would have to be shown first, e.g. with pull-down assays). This could be achieved by replacing one amino acid inside the binding pocket with a bulky amino acid. The modified gene would then be inserted into the genome of our cells, but not expressed right away. We wait for the cells to fully develop, silence the working copy of *SPTLC1/2* and instead express the engineered version. From that point on we would be able to observe the effects of the two subunits no longer being able to bind. We expect these results to be congruent with inhibition of dimer formation by our drug. These results will also validate a causal relationship between the observed effects (reduction in sphingolipid levels) and our proposed mode of action (inhibition of dimer formation).

If this experiment finds that the proposed mode of action does not inhibit ceramide synthesis significantly, other strategies could be employed. There are several other drugs which inhibit SPT by interfering with the enzymatic reaction rather than the formation of the complex[37]. However, the mode of action of these drugs was determined only after the discovery of their therapeutic potential and not by specifically screening for compounds which inhibited SPT.

To identify such compounds, we would adopt a functional assay for the screening. Specifically, we would look for compounds which improve survival of WT cells in a serine depleted medium, or C133W cells in normal medium. This would allow identifying compounds which inhibit the production of the toxic deoxyceramide

intermediates, as well as compounds with different modes of action. To identify compounds which specifically inhibit SPT we would then make use of mass spectrometry, once the number of candidate compounds is lower.

In vitro screening - primary assays

In this phase around 2600 compounds selected by virtual screening will be tested *in vitro*, in order to select a small number of promising candidates. The three main aspects that need to be verified are activity, physicochemical properties and toxicity.

Initially the compounds will be screened for solubility. The resulting compounds will then be screened for inhibition of the SPT dimer. The relationship between dimer formation and enzymatic activity will have already been established in the validation phase, allowing us to focus our initial screens on compounds that inhibit dimer formation. We made the choice to screen for dimer formation rather than measuring the sphingolipid levels directly as this allows higher throughput at lower cost.

The first screen will be performed cell-free, using a fluorescence polarization assay. The resulting compounds will be tested in human cells using a split luciferase assay. Only once the number of candidate compounds has been reduced significantly, we will test the effects of our candidates on sphingolipid levels directly in primary cells. This process should select a small number of compounds which will then be tested for cytotoxicity and intestinal permeability.

Solubility screen

The most reliable method to measure solubility (at a given pH and temperature) is the shake-flask method[38]. This consists in adding a surplus of a compound to a certain medium until saturation. Saturation is reached when the formation of a precipitate is observed. UV spectroscopy is then used to measure the concentration of the compound. Liquid chromatography-mass spectrometry (LC-MS) can also be used for compounds with poor UV absorption. The compounds that are soluble in the physiological pH range are allowed to move forward. As our virtual screening attempts to predict for solubility of the molecules we do not expect a large reduction in the number of compounds at this stage.

Fluorescence polarization assay

The around 2000 compounds that make it through the solubility assay will be tested for potency with a relatively simple but high throughput cell-free assay. Fluorescence polarization assays measure the interactions of labelled proteins by exciting the fluorophores with polarized light and measuring the polarization of the emitted light[39]. Specifically, molecules that rotate slowly emit light that is more polarized than the light emitted by fast rotating molecules. In our case if labelled *SPTLC1* binds *SPTLC2* it forms a heavier complex, slowing down rotation speed and leading to an increase in the polarization of the emitted light (Figure 5A). Therefore, the compounds can be screened for potency by selecting the ones that induce the lowest degree of polarization in this assay, indicating inhibition of the dimer formation.

An appropriate dye is chosen to obtain a good sensitivity, based on the weight of the monomers (Figure 16). To compare between the compounds, we define a score as:

$$S_{compound} = \frac{P_{negative\ control} - P_{compound}}{P_{negative\ control} - P_{positive\ control}}$$

Where the negative control is the mixture of labelled *SPTLC1* and *SPTLC2* in the absence of a compound and the positive control is the labelled *SPTLC1* alone.

This type of assay is indeed very convenient due to the low number of steps (mix-and-read) and its compatibility with high throughputs, but it is likely to return an optimistic list of candidates: since the library generated by the virtual screening should be biased for activity on the SPT dimer, we expect to find a relatively high number of compounds with some degree of effect. However, some of these compounds might not be able to permeate cellular membranes or might not work as well in a cellular environment. Therefore, it will be necessary to run a second, more physiologically relevant screen, on the compounds that give the most promising results in this assay. Indicatively we would select the compounds which score in the top 5% (around 100).

Split-luciferase complementation assay

In this step the pool of 100 candidate compounds resulting from the fluorescence polarization assay is screened again in a cell-based assay. Protein fragment complementation assays (PCA) are well characterized genetic techniques used to study protein-protein interactions in a cellular environment[40]. In general, all types of PCA involve fusing the two proteins of interest with complementary fragments of a third protein. When the proteins of interest interact, they reassemble the split protein, eliciting a measurable response (Figure 5B). We will make use of a split luciferase, an enzyme that emits light when supplied with the substrate luciferin.

In our implementation *SPTLC1* and *SPTLC2* would be fused respectively to the C and N terminal fragments of luciferase. For this assay we will use HEK cells, which are often chosen for these applications due to their propensity for transfection. The cells would be transfected with the constructs, overexpressed by a viral promoter to increase SNR.

By measuring the luminescence in the presence of the candidate drugs it will be possible to quantify the inhibitory effects of the compounds. Specifically, lower emission corresponds to a higher degree of inhibition and we can compute a score for the compounds defined as:

$$S_{compound} = \frac{L_{negative\ control} - L_{compound}}{L_{negative\ control} - L_{baseline}}$$

Where $L_{negative\ control}$ is the light emitted in the absence of any potential inhibitor, $L_{baseline}$ is the light emitted with no luciferase reaction (essentially zero) and $L_{compound}$ is the light emitted when the candidate inhibitor is added. At this stage we would chose a stringent cutoff to isolate a very small number of candidates. We would aim for around 5 compounds, keeping in mind that some of the hits might have a similar structure leading to even smaller number of independent candidates.

This assay can then be used again to find the IC_{50} of the selected compounds by creating the dose response curves.

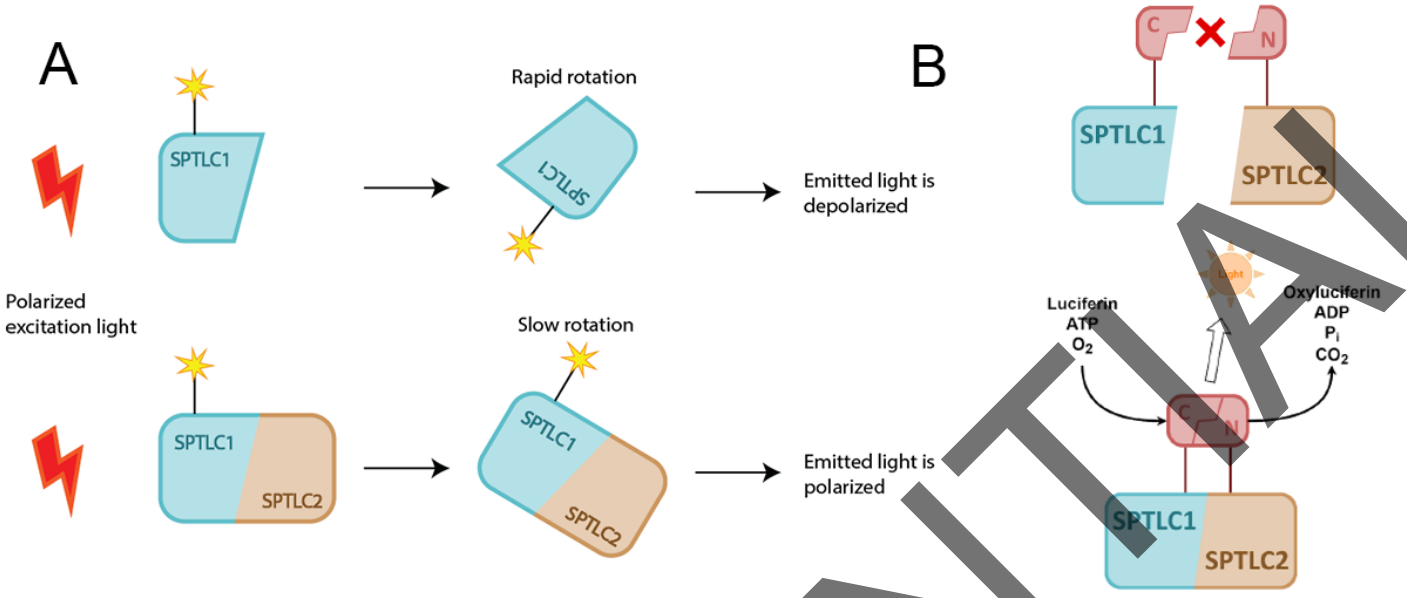

Figure 5 – Cell-free and cell-based assays to measure interaction between SPTLC1 and SPTLC2. A) Diagram of fluorescence polarization assay. Rapidly rotating fluorescently labeled SPTLC1 emits relatively depolarized light when excited with polarized light. SPTLC1/2 dimer rotates slower, leading to increased polarization of the emitted light. B) The scheme represents two subunits of the serine palmitoyl transferase long chain (SPTLC) enzyme, SPTLC1 and SPTLC2, as interacting proteins taking part in a PCA and respectively fused to the C-terminal fragment and the N-terminal fragment of the luciferase. The left panel symbolizes a non-interactive assay of SPTLC1 and SPTLC2, thus catalyzing no product through its unfused luciferase fragments, whereas the right panel depicts an interactive assay of the two subunits, in which the C- and N-terminals of luciferase fuse and take up luciferin, ATP and O_2 to catalyze the production of oxyluciferin, ADP, P_i, CO_2 and light, which can be assessed by luminescence ratio measurements.

Ceramide level measurement

The compounds that have been identified as inhibitors of the SPT dimer formation should be validated by measuring their effects on ceramide levels directly. In particular we want to quantify the effect of the drug candidates both in WT cells as well as in cells carrying the C133W mutation. Given the limited number of compounds at this stage we can make use of mass spectroscopy as described by *Kasumov et al*[41]. This method, which involves liquid chromatography followed by electrospray ionization tandem mass spectroscopy, is capable of measuring individual subspecies of sphingolipids. To this end our company will acquire a high-performance liquid chromatography (HPLC) system and a mass spectrometer, since this type of measurement will also be used in the *in vivo* phase.

Using these tools, we will analyze the levels of all sphingolipid species that are part of *de novo* ceramide synthesis (3-ketosphinganine, sphinganine, dihydroceramide, ceramide) as well as their toxic deoxy counterparts. Given that our compounds should only affect the *de novo* pathway we would expect to only see a partial decrease of ceramide levels, both in WT and C133W cells, compared to untreated cells. Conversely we would expect to see a sharp decrease of deoxy-3-ketosphinganine, deoxysphinganine and deoxydihydroceramide in treated C133W cells. Compounds that do not elicit this response will be rejected.

Cytotoxicity screen

After performing the potency assays, the hits will undergo the first of several **toxicity screenings** to complement the virtual toxicity predictions proposed above. It makes sense to test toxicity as soon as possible, as it is the main criterion for rejecting a drug in development[42]. Toxicity is a measure of the harm and damage caused by a compound that is in contact with living matter. In the case of our drug, which is administered to a patient for an extended period of time (months or even years), little to no toxicity is permitted to remove the chance of any long-term side effects. Several kinds of toxicity are distinguished, of which cytotoxicity gives the most immediate feedback. All compounds showing any cytotoxicity will be excluded from further development processes. To measure cytotoxicity, we will investigate the following qualities in a high throughput setting:

- Metabolic cellular activity by means of an **MTT assay**[43]: Assay with a colorimetric readout based on absorbance values. Tetrazolium dye (MTT) is added to the cell culture and will be reduced to a purple product by the mitochondria of viable cells.
- DNA proliferation by means of a **BrdU assay**: The pyrimidine analog bromodeoxyuridine (BrdU) is added to the cell culture and will be integrated by dividing cells into their genome instead of the naturally occurring base thymidine. Antibodies are then used to quantify the amount of integrated BrdU, thus measuring cell proliferation. The readout is also colorimetric because horseradish peroxidase is employed as a reporter.
- Production of ROS/RNS by means of **EPR spectroscopy**[44]: Reactive oxygen species (ROS) and reactive nitrogen species (RNS) are free radicals produced by biochemical reactions. They are usually neutralized via reduction inside the cell, but a drug might disturb this equilibrium and lead to their accumulation. This is dangerous because they may react with lipids, proteins or DNA and induce structural changes, rendering the molecules dysfunctional. Electron paramagnetic resonance (EPR) spectroscopy allows detection of unpaired electrons and thus free radicals.

The toxicity screens will be repeated for different concentrations of the drug, as we expect the drug to have an impact on the measured parameters since it is targeting an important metabolite. We will perform a dose escalation protocol, where absence of the drug will serve as control. The maximum toxic dose will exceed the IC_{50} value. Only compounds for which no cytotoxic effect is observed below the IC_{50} dose are selected.

Specificity screen

To further keep adverse drug reactions at a minimum, specificity screening is performed in parallel to cytotoxicity screenings[45]. This is usually outsourced to a company specializing in the test. It aims to expose the drug to a likely set of enzymes, lipids, etc. present in the human body and check for off-target interactions with any of these[46]. The drug should only interact with our specified target, namely the SPTLC1/SPTLC2 complex, any other interactions are dangerous and have to be avoided.

Only drug candidates that have passed all of the above tests will be considered in the further stages. At this point, the pool of candidates is reduced to a few hits. Before proceeding, we will analyze the **structure-activity relationships** (SAR) into which we can divide the hits[47] and rate them according to our desired properties and obtained screening results. Following a process coined **hit expansion**, the three best SAR families will be optimized for e.g. improved solubility or binding affinity to the target by repeating the aforementioned primary assays on structural analogs. These structural analogs can be synthesized based

on fragments of the compounds exhibiting the best SAR, in what is commonly known as the **SAR by catalog** approach[48] in the industry. The final best hits will be termed leads and proceed to testing in the next stages.

In vitro screening - secondary assays

The identification of the best leads will be performed by more advanced toxicity screens and other *in vitro* methods to decide which compounds will make it further to *in vivo* validation.

Intestinal permeability screen

Orally administered drugs are mainly absorbed in the intestine. Not all compounds have the same permeability, mainly due to size and shape, but also based on other factors like efflux, transporters, hydrophilicity, lipophilicity. To select the compounds with the highest permeability through intestinal cells, and therefore highest bioavailability, we will conduct a Caco-2 permeability assay[49]. A monolayer of Caco-2 cells mimics the properties of the intestinal mucosal epithelium, making them a good model for the assay. Liquid chromatography-mass spectrometry and LC-tandem mass spectrometry is used to measure compound concentration on the apical and basal side of the cell layer.

Mutagenesis screen

Unknown compounds may interact with DNA inside the cells and induce spontaneous mutations. Mutations will be inherited by daughter cells and cannot easily be detected nor reversed. They can cause enzymes to change structure with drastic consequences in certain cases[50], such as cancer. Mutagenesis screens allow for detection of compounds eliciting such changes, of which there are several types with appropriate screens listed below.

- Point mutations/insertions/deletions are detected by means of an **Ames test**[51]: *Salmonella Typhimurium* strains are genetically engineered to have a point mutation at varying positions in a gene responsible for *de novo* synthesis of the amino acid histidine, making them dependent on externally acquired histidine[52]. The drug is added to the culture and the colonies are screened for an increase in spontaneous mutations that make them regain their histidine independence. This increase can be compared to the administered dose of the drug to get a quantitative readout of mutagenicity.
- Chromosomal aberrations and changes by mean of an ***in vitro*** **micronucleus test**[53]: Micronuclei denote the chromosomal remainder when unequal amounts of chromosome are split in cell division, with the aberrant chromosomes visible under light microscopy in the cytoplasm. The *in vitro* version of the test in mammalian cell culture (for instance in human lymphocytes) can give first insights for unsuitable compounds, but systemic mutagenicity has to be evaluated in animal models nonetheless.

Synthetic lethality screen

To ensure that our drug will not interfere with other common types of treatments or the Standard of Care for our target diseases, we will perform a synthetic lethality screen[54]. This is a common procedure for pharmaceutical companies[55] and is dictated by some EMEA[56] and FDA[57] guidelines. For this screen, cells are exposed at the same time to our drug and another molecule that could be common in other therapies of our target patients. A screening library has to be generated and must include common FDA-approved drugs and specific compounds used in treatments to which our target patients are susceptible. Cell viability is assessed a few hours after administration of both drugs to the culture - in case of cell death, the corresponding

drug pair is synthetically lethal, and the drugs should not be consumed in parallel. Some more tests could be imposed by FDA; genotoxicity assays with two drugs are generally not required. The test is normally done in yeast cells, but human cell lines may also be used. The main problem of this type of screen is given by the enormous amount of possible drugs and dosage combinations to test. Several methods aiming to reduce the complexity or to introduce a methodology in the choice of the tested couples exist. Among them, some QSAR machine learning algorithms are particularly interesting since they allow identify *in silico* the potential toxicity combinations that can then be tested *in vitro*[58]. Alternatively, the library could be generated from the 100 most administered drugs worldwide.

In vitro embryotoxicity screen

To assess the drug's possible side effects on a developing fetus or embryo, an embryotoxicity screen has to be performed. The *in vitro* version of the screen uses permanent mouse embryonic stem cell lines[59] (mESC) and exposes them to the drug at different stages of embryogenesis. Important metrics are cell differentiation and correct division. The screen will focus on the development of cardiomyocytes, stem cells and fibroblasts for analysis.

Microsomal stability assay

In order to mimic the *in vivo* processing of a wide array of drug candidates and assess their toxicity, as well as their pharmacodynamic and pharmacokinetic properties, it is necessary to realize an early-stage *in vitro* assay that takes into account the metabolization of these compounds by the liver, as it represents the main site for drug metabolism in the human body[60,61]. The microsomal stability assay aims to reproduce mouse, dog or human liver-like environments by presenting automated high throughput procedures for the setting up of parallel incubation mixes (prepared with buffer, drug solution, cofactors and microsomes extracted from the target organism). Detection of the compounds is performed through liquid chromatography tandem mass spectrometry (LC/MS/MS) and the subsequent raw data processed with statistical treatment. It is thus possible to elicit an output with compounds presenting optimized properties in regard to criteria such as bioavailability or non-toxicity.

Photoreceptor study in retinal organoids

Retinal organoids are the result of human pluripotent stem cells (hPSC) growing into a three-dimensional structure after appropriate cell differentiation[62]. They can be used to demonstrate the deleterious effect of deoxysphingolipids bases on photoreceptors. These organoids are stratified and contain most of the major neural cell types found in the retina. We will cultivate retinal organoids in an environment deficit of serine or its precursor. These organoids will then be treated with our drug at different concentrations and photoreceptor death is measured after several days. Significantly reduced or no photoreceptor loss is expected in organoids treated with our drug, but not in the control.

In vivo validation

The next stage in the development process involves animal testing which will be performed in compliance with Good Laboratory Practices as defined by the European Medicines Agency[63]. Based on *in vitro* data, *in vivo* tests aim to provide proof-of-concept of an *SPTLC1-2* complex inhibitor for both HSN1 and MacTel

conditions. Our results will be submitted in a Clinical Trial Application to the Regulatory Authorities and Ethics Committee to get the approval for our clinical trials.

In vivo validation will test and narrow down the 5 selected compounds that passed the *in vitro* screening. Compounds are first tested on healthy mice in order to establish the pharmacokinetic and pharmacodynamic (PK/PD) profile of the drug and its toxicity. These parameters will lead to the determination of the optimal dosage that is used during the efficacy assessment and establishment of the pharmacokinetic profile on mouse models. In this proposal, two mouse models with different genetic backgrounds are chosen for the efficacy study. Eventually, after successful validation of one compound, toxicity tests and optimal dosage determination are again performed on dogs to further characterize the compound in a non-rodent species.

Pharmacokinetic (PK) and pharmacodynamic (PD) profiling

PK/PD profiling allows to decide a candidate compound that can proceed into the first human study and to determine its optimal oral dosage. Absorption, distribution, metabolism and excretion characteristics of the 5 selected compounds are first assessed in healthy mouse models with heterogeneous genetic background.

For cost and time saving reason, a rapid assessment of compound exposure (RACE) is performed. This PK screening method determines PK attributes of chemical probes[64]. A single dose (10 mg/kg) of compound is administered orally by gavage using a stomach tube to 2 mice. After 20 and 120 minutes, blood samples are collected, and compound concentration is analyzed by liquid chromatography mass spectrometry (LC/MS/MS). The concentration in plasma versus time curve gives a quick overview of compound exposure (area under the curve AUC) providing a first ranking of selected compounds.

Further pharmacokinetic analyses are performed on compounds showing encouraging PK profiles. Three different doses, based on *in vitro* assays, are received by oral gavage in groups of 6 mice. Blood samples (30 µl) are collected for each mouse at 8 time points (15 min, 30 min, 1 h, 2 h, 4 h, 8 h, 16 h, and 24 h). Each mouse sample is centrifuged and diluted appropriately to ensure concentrations in the dynamic range of standard curve (1-5000 ng/ml). Analysis by LC/MS/MS provides time course of compound plasma concentration. PK parameters are calculated using WinNonlin software: maximum concentration achieved (C_{max}), time for maximum concentration (T_{max}), area under the curve (AUC), half-life ($t_{1/2}$), oral bioavailability and clearance (C_L)[65,66].

To characterize tissue distribution of the compounds, mice are sacrificed at T_{max} and specific organs are analyzed by mass spectrometry; the brain to check if the blood-brain barrier has been crossed, the dorsal root ganglia[67] and eyes as our drug target sites, and the liver and kidney as key organs for metabolism and excretion. Absorption by the intestines should be positive as it increases bioavailability of our oral drug. The apparent volume of distribution can be calculated through the equation:

$$V_d = \frac{Amount\ of\ drug\ in\ the\ body\ [\mu g]}{Plasma\ concentration\ [\mu g/mL]}.$$

To investigate more detailed quantitative information about metabolism and excretion routes, selected compounds ^{14}C radiolabeled undergo a full mass balance study (MBS). Radioactive dose is based on PK properties of the previous experiment, it generally ranges between 1.5-100 µCi/kg. Quantitative whole-body autoradiography (QWBA) determines radiolabeled compounds distribution in various tissues and their level of radioactivity is identified by liquid scintillation counting (LSC)[68]. This technique mixes the radioactive samples with a liquid scintillator and counts the resultant photon emissions. The experiment lasts more than

5 plasma half-lives of the parent compound. At 5 different time-points, plasma, urine and fecal samples are collected and analyzed[69]. Compounds are screened according to their PK characteristics; large Vd, good absorption, not too rapid elimination and high bioavailability are desired.

Further studies of the 3 more convincing compounds are conducted to investigate their effects on ceramide level. PD studies last 5 days, each of the 3 candidate compounds is administered orally in mice fed with 50:50 radiolabeled serine and alanine diet. Since inhibition of *SPTLC1-2* complex is expected to reduce incorporation of alanine in sphingolipids, the radioactivity level in ceramides is measured. Furthermore, ceramide level is measured to check compensation of synthesis by other pathways than the *de Novo* one.

Eventually, based on PK/PD assays, the most promising compound is selected to progress through the development pipeline. The two other compounds are left on the wayside but kept in case of any unexpected event that could be encountered with the drug candidate chosen. Moreover, the PK/PD ratio allows to determine the effective dose of the promising compound which is determined as the highest possible but still tolerable dose level with respect to a pre-specified clinical limiting toxicity. This effective dose is used for further test of toxicity and efficacy.

Toxicity assays

To evaluate the toxicity of our compound we perform several types of toxicity tests that are essential to assure the safety of our compound(s) before the clinical study. Those tests are achieved following the ICH safety guidelines[70] for the testing of chemicals.

Several tests are performed in parallel; 4 groups of 20 healthy mice (10 males and 10 females) receive different doses of treatment for 3 months (acute administration), 6 months (sub-chronic administration) or 12 months (chronic administration). The first group receives a placebo (null dose), the second group an effective dose based on previous PK/PD ratio, the third one receives half of the toxic dose (5 times the effective dose) and eventually, the fourth one receives a toxic dose (10 times the effective dose).

To test for mutagenesis *in vivo* at the chromosome level, a micronucleus assay is performed, looking for any chromosomal damage. We can well visualize micronuclei in erythrocytes because they lack a main nucleus. An increase in the frequency of micronucleated polychromatic erythrocytes in treated animals is an indication of induced chromosome damage. Cytokinesis-block micronucleus (CBMN) is used as a method of detection[71] . In this method Cyt-B is used to block the nuclear division of the cell as it is an inhibitor of actin polymerization. By scoring the MNi in the binucleated cells of treated mice we can assess the chromosome damage due to our inhibitor. To assess the mutagenic potential, the *in vitro* Ames test can also be performed on cells extract from target tissues. The test is the same as performed in the *in vitro* part and we can use liver or kidney cells, which are the mains organs involved in the metabolism of the drug. When the strains are grown on a minimal media that does not contain histidine, the strains are not able to grow. By adding a mutagen agent, it will recombine and causes mutation in the region of histidine dependence and reverts the phenotype making the strains histidine-independent which will then be able to form colonies. If after adding our dimer inhibitor, the number of colonies stays constant, we can conclude that it is not mutagenic[72].

The immunotoxicity is also tested by measuring the level of immune cells in the blood of treated mice during the treatment. Suppression of the immune response can lead to decreased resistance to infectious agents or tumor cells whereas enhancing the immune response can exaggerate autoimmune diseases or hypersensitivity. In a first test, hematological changes are assessed by measuring the level of granulocyte,

leukocytes and lymphocytes. After a certain period of treatment, the mice are sacrificed and histological measurements are performed in lymphoid organs (such as spleen, lymph nodes, or thymus).

Later on, cancerogenesis is evaluated by looking for any tumor tissue during and after a period of 18 months of treatment (corresponding to a period of treatment even larger than the chronic period of test). For this treatment 20 mice are recruited (10 males and 10 females). If no tumor tissue is observed during this time, the mice are sacrificed and undergo necropsy at the end of the test. Specific tissues such as liver kidney, dorsal root ganglia and eyes, are targeted for histopathological studies with particular attention given to abnormal masses and lesions. In the case where there is no sign of tumor, the compound is considered as safe and non-carcinogenic.

Finally, reproductive and developmental toxicity screening assay is performed by mating 10 treated males and 10 treated females. A developmental toxicity/embryotoxicity study is performed by taking 10 different pregnant mice. The treatment is administered between the 8th and 14th day of pregnancy and embryonic lethality is monitored. On the 21st day of the study, a caesarean section is performed and parameters such as limb malformations, exencephaly, open eyelids as well as the mortality and the numbers of dead and live pups are noted to assess for any developmental problem[73] .

Some mice are, in parallel to the main toxicity test, subject to a period of recovery of 1 month without treatment and are then sacrificed to look for any organ damage by histology test. LC/MS would also be performed to quantify the level of remaining compound in the blood. Recovery of the mice is indicative of non-permanent toxicity of the compound.

After testing for any potential toxicity on our remaining compound, the efficacy on HSN1-like and MacTel-like mouse model is established.

Efficacy and pharmacokinetics on mouse models

Mouse models

Two mouse models are chosen to perform the efficacy and PK assessments. The first model is a non-mutant, outbred strain fed with a serine- and glycine-depleted diet. This diet induces a decrease of serine levels that cannot be compensated by the conversion of glycine into serine, and thus leads to the preferential binding of alanine instead of serine to the SPT enzyme[74]. The alanine then induces production of deoxysphinganine, whose levels have been found to be negatively correlated to serine levels in those mouse models. Eventually, the neurotoxic compound deoxydihydroceramide is synthetized from deoxysphinganine, leading to the development of the diseases. Indeed, results show that after ten months, the mice develop symptoms similar to both MacTel and HSN1 symptoms. In particular, deficits in the photopic and flicker responses and an elevated thermal latency threshold are observed[Erreur ! Signet non défini.]. As this model reproduces the molecular and clinical features of both diseases while representing a wide range of genetic backgrounds (no specific variants), it is therefore a suitable model. Indeed, a majority of the MacTel patients do not have a specific mutation inducing the disease[75] but all have reduced serine level leading to it. On the contrary, HSN1 is induced by a mutation either in the *SPTLC1* or *SPTLC2* gene leading to the dysfunction of the SPT enzyme. In this case, the low-serine mouse model is also suitable as it mimics the same binding of alanine instead of serine to SPT, observed in the neuropathy, even if the causes of this binding are different. Moreover, as HSN1 patients do not all have the same mutation, the first model would again represent the genetic

heterogeneity among the patients. However, as the most common mutation observed in HSN1 patients is *SPTLC1*^{C133W}, it has thus been decided to use a second mouse model for further validation of our inhibitor.

The second mouse model proposed for the *in vivo* validation is the mutant strain bearing the *SPTLC1*^{C133W} mutation[76] in which the onset of the neuropathy is at 14 months of age. The symptoms associated with this model are an increase in long chain ceramide (C16:0 and C18:0), increase in deoxysphingolipids levels, sensory and mild motor impairment while displaying unaltered canonical activity[77]. This model is expected to give us more insights into the mechanism of inhibition of the dysfunction SPT enzyme that could not be characterized with the low-serine mouse model. This model is also suitable for the characterization of MacTel as HSN1-affected patients often develop the macular disease as well[78].

Experimental Design

The efficacy assessment of our compound is performed on groups of 20, 14 months old, mice (10 females and 10 males) of each of the two strains (sample size determined through power analysis[79] using deoxysphinganine level data in serine-depleted and control mice[12]). 10 mice (5 females and 5 males) of each strain are given the drug assigned to the group while the remaining mice are given the solvent used to dilute the active compound. The mice are treated for 6 months. A third group of 20, 14 months old, control mice is included. As for the mouse models groups, the control group is separated in two groups of 10 mice, one is given the drug while the other is given the solvent. The control group is used to assess the effects of the drug on healthy, aged-match, mice as the toxicity tests are performed on young mice only.

Throughout the treatment, deoxysphinganine, deoxydihydroceramide and ceramide levels are measured in the plasma using LCMS[80] and sphingolipid and ceramide species are determined using SRM[12]. Upon successful treatment, deoxysphinganine and deoxydihydroceramide levels are expected to decrease while ceramide levels should remain within a physiological range.

The efficacy of the compounds for the treatment of MacTel symptoms is evaluated through Optical Coherence Tomography-Angiography (OCT-A) and Electroretinogram (ERG). OCT-A is a non-invasive imaging technique used to characterize the retinal perfusion[81]. ERG measures the electrical activity of the retina in response to a light stimulus. The results of those tests for treated mice are expected to approach physiological responses.

Eventually, the efficacy of the compounds for the treatment of HSN1 symptoms is evaluated through electromyography (EMG), nerve conduction velocity (NCV) testing and hot plate test to measure the thermal latency threshold (TLT). The results of these tests for treated mice are expected to show an improved muscle fibers recruitment, an increase in nerve conduction velocity and a decrease in the thermal latency threshold in comparison to untreated mice.

The main advantage of all these tests is that they are translatable to humans. Figure 6 summarizes the experimental design discussed above.

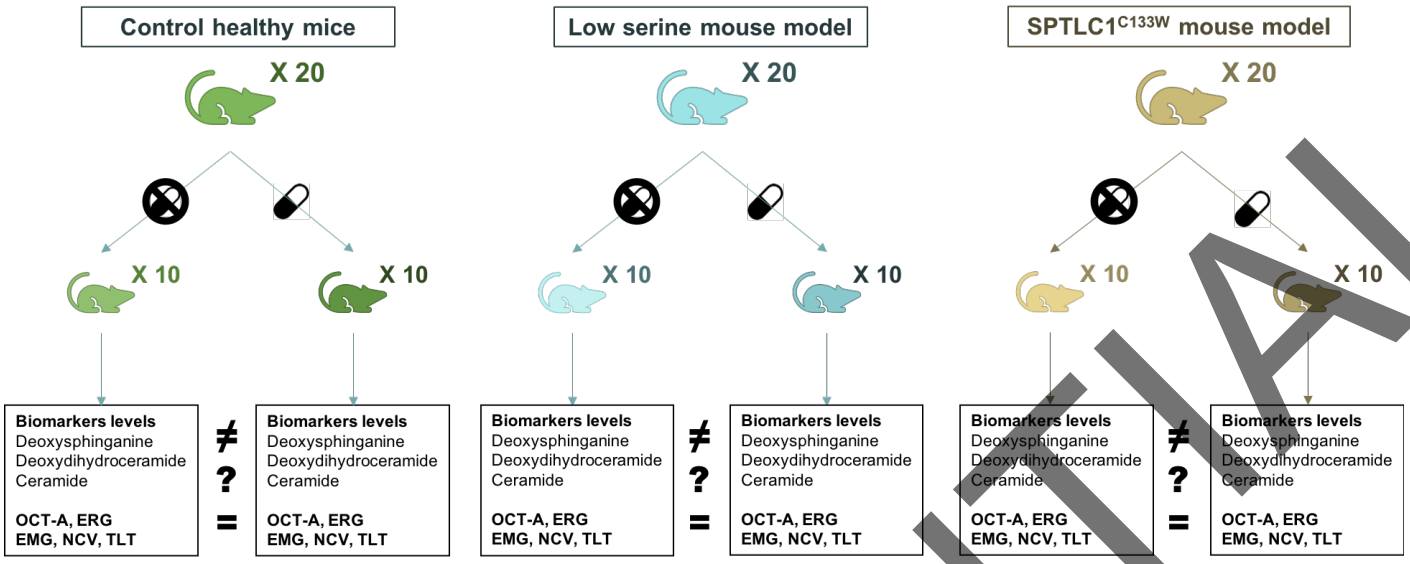

Figure 6 - Experimental design to test 1 compound. 20 mice of each model + control mice are separated into two groups of 10 mice and only one of those two groups receives the drug. Efficacy is evaluated through biomarkers levels and disease-specific tests and the results are compared between treated and untreated mice; a significant improvement in the test's results of treated mice is a proof of the efficacy of the compound to treat the symptoms of one or both diseases.

PK/PD profile and toxicity assays on healthy dogs

Safety evaluation prior human trial is performed on non-rodent species in accordance to the ICH guideline S4[70]. PK evaluation and long-term toxicology studies (9 months) are performed on dogs. 3 groups of low, clinical and high daily oral dosing and one control group are monitored. Integrity of the nervous system, cardiovascular and respiratory systems are controlled. To assess PK profile blood samples are collected and a full MBS is performed (see section PK/PD).

Based on PK/PD profiling and toxicity assays a single investigational product is submitted for clinical authorization. The preclinical toxicity testing helps to calculate the No Observed Adverse Effect Level (NOAEL) which is needed to initiate the clinical evaluation.

Clinical Trials

Phase I

The main aim of phase I being to assess the toxicity of the drug, we will first perform a dose escalating study to determine the Maximum Tolerated Dose (MTD) in humans. In order to define an appropriate starting dose, the No Observed Adverse Effect Level (NOAEL) found in both mice and dogs is used. Firstly, the Human Equivalent Dose (HED) in mg/kg is calculated, which is a conversion of the NOAEL [mg/kg] based on the body surface area with the following formula[82]: $HED = NOAEL_{animal} * (km_{animal}/km_{human})$, km being defined as the body weight divided by body surface area [kg/m²]. Then, for safety reasons the lowest dose of the two is retained and is subsequently divided by a safety factor of 10 (i.e. the default factor usually used) to obtain the Maximum Recommended Starting Dose (MRSD).

To conduct this study, which is expected to last at most 1 year, 20 to 40 healthy volunteers are enrolled. Since these subjects will not receive any potentially therapeutic benefit, they must be exposed to minimal risk, thus strict exclusion criteria are adopted. Indeed, vulnerable subjects such as children, pregnant women or elderly are excluded, as well as subjects under ongoing treatments, or abusing any kind of drugs.

In the single ascending dose study, the standard 3+3 design[83] will be used. Firstly, the MRSD is administered to 3 healthy subjects. In case no toxic effect is observed, another group of 3 subjects gets a higher dose and the study goes on (Figure 7). However, if one subject experiences a toxic effect the same dose has to be tested again on 3 different subjects. The trial then stops if in this other group an adverse effect is observed as well. In addition, if such a toxic effect is present in more than one subject of the same group, the dose escalation study directly stops and the MTD retained is the previous dose tested. Note that smaller increments can be adopted around the expected therapeutic range, in order to obtain the most fine-tuned and representative MTD value.

Afterwards, a multiple dose escalation study will be conducted to observe potential adverse effects after repeated exposures to the drug, again using the 3+3 design (Figure 8). The administration of a dose to a group for one month is always followed by another month of washout period, to make sure no toxicity is observed before giving a higher dose to the next group.

	Day 1	Day 3	Day 5	Day 7	Day 9
Dose group 1	X = MRSD				
Dose group 2		2X			
Dose group 3			3X		
Dose group 4				4X	
Dose group 5					5X

Figure 7 - Single ascending dose study

	Month 1	Month 2	Month 3	Month 4	Month 5	Month 6
Dose group 1	MTD * 50%	Observation phase				
Dose group 2			MTD * 75%	Observation phase		
Dose group 3					MTD * 100%	Observation phase

Figure 8 - Multiple dose escalation study

In order to determine when an escalation study has to stop, the safety is assessed in various manners. Vital signs, physical examinations, electrocardiogram, blood samples, blood pressure and pulse will be controlled at each visit before and after the administration of the drug. More specifically, circulating levels of deoxysphinganine, deoxydihydroceramide are measured from the plasma, and ceramide levels are checked as well given that they are expected to be maintained within a normal physiological range. Adverse events will be reported by the volunteers during the whole duration of the treatment and during the month of observation. If no major problems are detected during this phase, the highest dosage permitting to have no adverse events will be chosen and a phase II will be performed on HSN1 and MacTel2 patients.

Phase II

Once the safe dosage range is determined in Phase I, our study will proceed with Phase II. The goal of this part consists in establishing if our drug has a sufficient outcome in order to go through further studies in Phase III. In this phase it is important to detect the best drug dose to optimize the relationship between safety and efficacy. L-serine supplementation is currently ongoing clinical trials for HSN1 treatment[84], this can greatly facilitate the approval of the clinical trials on our drug and is also helpful to get insights on measuring efficacy.

Phase IIa

For the first part of Phase II we will recruit 12 HSN1 patients with the specific mutation *SPTLC1*^{C133W} which is the most common one. Since the prevalence of this disease is rather low (~2/1'000'000[7]), a multi-center study with 4 centers is planned, such that each center will have 3 patients at charge. Considering the prevalence of the disease and targeting big cities, it will be possible to obtain the number of patients required. The participation to the study will be limited by classical exclusion criteria in clinical studies.

In our double-blind, placebo-controlled cross-over study, patients will be randomly divided into 3 groups of 4. Each group will go through a 6 months testing period three times, each time followed by 2 months wash-out period as shown in Figure 9. This way we would be able to test 2 different doses (the one determined in phase I and 50% of it) against the placebo taking intraindividual variability into account.

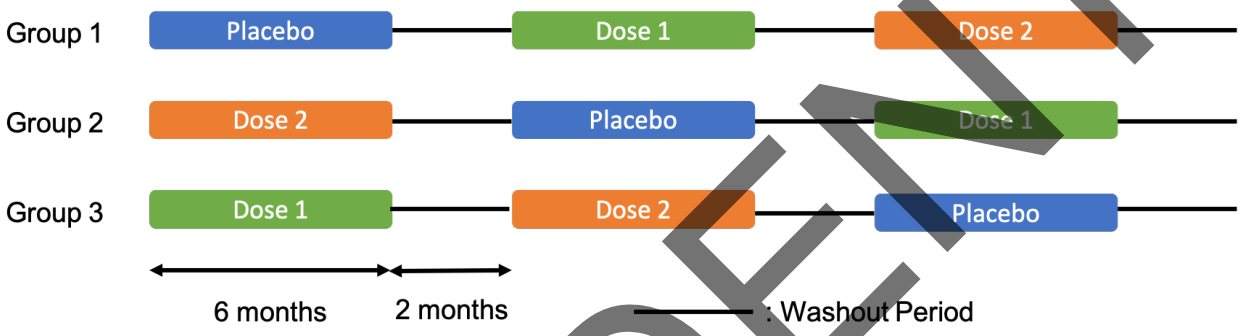

Figure 9 - Placebo-controlled cross-over study pipeline

To assess the efficacy of the drug, a determined list of tests will be performed at the beginning and the end of every testing period. The same biomarker measurements and tests as in the animal models from preclinical *in vivo* trials will be measured, as well as some other measures used in the L-serine supplementation study such as Charcot Marie Tooth Neuropathy Score (CMTNS), Autonomic Function Testing (AFT) and Composite Autonomic Severity Score (CASS).

On the side of the efficacy test mentioned above, the same safety checks as the one listed in Phase I will be performed on a regularly basis (every month). Also, participants are specifically asked to report any observed adverse effect or unusual condition.

Phase IIb

If the results of phase IIa are satisfactory, we will be able to use the orphan disease status of both HSN1 and MacTel to get a fast track in this phase. Since the genetic disease model is clearly defined and there is almost no variance regarding cause of disease, we expect facilitated approval to extend our clinical trials to HSAN1 or MacTel2 not caused by the *SPTLC1*^{C133W} mutation. This is supported by one of the mouse models used for animal trials which only has low serine levels as disease cause.

Again, we aim to recruit 12 participants with at least 6 HSN1 and 6 MacTel2 patients (knowing that a patient can exhibit both diseases). This phase will use the same protocol as before except that only the best dose will be tested against the placebo. All the tests mentioned in Phase IIa will be performed again to assess HSAN1 evolution as well as the eye imaging test used in mouse model for MacTel2 evolution.

Phase III

Assuming sufficiently satisfying results during phase II trials, our drug will be accepted to enter phase III trials. The aim of phase III is to finally assess the drug's efficacy for a longer period of time, which we expect to last about 3 years, and with a considerably larger number of subjects with respect to the previous phases to check for uncommon and/or long-term side-effects. Since the prevalence of both the HSN1 and MacTel2 disease is very low, having 200 patients enrolled in this phase would already be considered satisfying. In addition, note that no other treatments are available yet for the same diseases, thus no comparison can be made in terms of drug efficacy.

Phase IV and Extension to different neuropathies

Clinical trials phase IV consists of a post-marketing surveillance trial, aiming to keep investigating the drug safety and efficacy even after the FDA approval. In addition, the use of our drug can potentially be expanded to treat other kinds of neuropathies. Indeed, it was recently shown that paclitaxel, one of the most commonly used drugs for the treatment of solid tumors acts as an up-regulator of SPT[85]. It causes an increase in 1-deoxysphingolipids levels, correlated with the incidence of paclitaxel-induced neuropathy, which can lead to the obligation of lowering the chemotherapy dose treatments for those patients. Another study showed that the decreased L-serine levels play a key role in paclitaxel-induced peripheral neuropathy[86]. Also, the same relation between deoxysphingoid bases accumulation[87] and low serine levels[88] has been shown for diabetic sensory neuropathy which is the most common chronic complication of diabetes patients. Thus, since in both cases there is some evidence that the diseases can be caused by the abnormal production of deoxysphingolipids due to the low serine levels, we expect that giving our drug to patients under chemotherapy or diabetic diagnosed with peripheral neuropathy will lead to the same effects as in the HSN1 patients (i.e. the reduction of deoxysphingolipids-induced neurotoxicity).

Conclusion

Reduction of toxic deoxysphingolipids by inhibition of the SPTLC1/SPTLC2 complex appears to be a key strategy to treat patients affected by MacTel and HSN1. Since this treatment can greatly increase patients' quality of life, our whole drug development process is centered around it. The first stage in the process, virtual screening, allows a selection of 1000 compound based on physical properties. This pool of candidates is reduced and optimized with *in vitro* toxicology and activity tests. Further studies on mouse models examine PK/PD properties and *in vivo* toxicology of the 5 selected compounds. Efficacy of the 3 most promising candidates is assessed *in vitro* allowing the evaluation of optimal dose. Based on *in vivo* characteristics, the most appropriate drug is selected and evaluated in humans to study its efficacy in patients. Clinical condition improvements can then lead to marketing authorization of our drug. Post marketing surveillance follows patients many years after the end of clinical trials to ensure no adverse effects nor any long-term toxicity.

Looking beyond treating MacTel and HSN, our drug could potentially have more diverse applications. Low serine levels inducing alanine substitution in sphingolipid synthesis is observed in other pathologies such as diabetic neuropathy or ischemic stroke.

Recently, a number of studies showed that tissue damage due to anoxia following ischemic strokes are linked to the abnormal production of deoxysphinganine by SPT, because of a substrate switch from serine to alanine[89]. Although at this stage it is too early to plan other clinical trials for further extensions of our drug, in the future we believe that it has the potential to be used as a preventive therapeutic approach to limit the

tissue damage after a stroke, which would represent a real breakthrough considering that stroke is one of the most common causes of death worldwide and has no effective treatment to date. Our drug compound is thus not restricted to the conditions MacTel and HSN1 and offers promising extension prospects.

Supplementary information

Virtual screening methods and software description

1. STRING interactions analysis:

STRING[90] is a widely used online platform allowing to build protein-protein interaction networks considering functional and/or physical interactions. In this proposal, a network is generated for the human SPTLC1 considering experimental, co-expression, co-occurrence and database sources. Results are reported in Figure 10 and Table 1.

2. HADDOCK docking analysis:

Active and passive protein-protein surface residues are predicted with the experimental data-driven *CPORT* (Consensus Prediction Of interface Residues in Transient complexes) algorithm[91] and used as restraints inputs for *HADDOCK 2.4*[92]. Active residues are defined here as residues involved in the interface between two proteins. A penalty is introduced by *HADDOCK* for the active residues not at the interface of the protein. Passive residues can be involved in the binding interface but are not subjected to any penalty since considered having a minor importance.

HADDOCK 2.4 algorithm provides docking predictions driven by experimental data and allowing proteins flexibility. The simulations consist in an iterative approach where several conformations are tested, initially considering protein as rigid bodies, then introducing some degree of flexibility and finally adding water as solvent for a fine-tuning of the predictions. 10400 conformations are tested in total for each run. For our analysis, to improve accuracy, structures are not coarse-grained into Martini models currently used in the field of molecular dynamics. All the other parameters are the default proposed ones.

The protein flexibility allowed by *HADDOCK 2.4* is well visible in Figure 13, where small differences are visible between the two aligned SPTLC1 domains.

3. Visualization and mutation introduction:

The point mutation is introduced in the SPTLC1 .pdb file with the PyMOL[93] *rotkit.mutate* script. All the 3D molecular visualizations are generated with PyMOL.

4. Polar contact sites determination:

From the docking simulation results, polar contact sites are determined with *PDBsum*[94], a database providing a summary of the 3D structure properties of a *.pdb* file. Only residues involved in H-bonds are considered here. Results are reported in Figure 12.

5. LEA3D virtual screening:

To select the contact residues targeted by our candidate drug, a very simple clustering strategy is proposed here. A residue is selected in a way that a radial spatial cluster centered on it and potentially including other residues forming H-bonds (in both WT and mutant SPTLC1) is created. In each cluster the presence of at least one WT residue is ensured. A very simple assumption is made here. Since the average contour length per amino-acid is 4 Å (± 0.2 Å)[95], using a binding site radius of X Å would allow to potentially include in it the $N = \frac{(2X/4)-1}{2} = \frac{2X-4}{8}$ neighbor residues. This criterium implies chains linearity but it is selected to maximize the clusters sizes reducing by this way the number of simulations. A radius of 10 Å is chosen and virtual

screening simulations are run for the residues at the center of each cluster, allowing radial binding site flexibility around it.

LEA3D is the genetic algorithm selected for screening. Optimal molecular candidates are generated by linear combination of experimentally retrieved fragments, ensuring the construction of realistic molecules. Druglike fragments have been selected as being part of proven drugs to increase the generated candidate's likeliness[96]. Docking is simulated with *PLANTS* algorithm[97]. The global scoring to be maximized is a combination of molecular properties (Table B), each weighted according to its estimated relevance and according to a docking score. The weights and the constraints applied on the molecular properties are selected to maximize the drug-likeness following the classic Lipinski's Rule of Five (LRO5)[98], the Veber's rule[99], the Rule of Tree (RO3)[100] and some observations summarized by *Lepre et al.*[101] and *Xe et al.*[102].
A maximum of 51 genetic generations with 40 mutated molecules each and binding site centered on the selected residues and with a maximum radius of 10 Å are selected as parameters for the simulations. This allows for each run to evaluate a total of 2040 molecules, of which the best 51 are selected. An example of the score evolution over generations is provided in Figure 14.

Retrieval of all the results was possible thanks to a custom web-scraping python script, allowing to additionally introduce a specific nomenclature for the files (and therefore for the molecules), comprising the name and position of the residue selected for each simulation, its ranking among the output molecules and its *LEA3D* global relative score. A graphical summary of the results is provided in Figure 15. Chemical structures representations of some of the selected molecules are obtained with the *obabel* script[103].

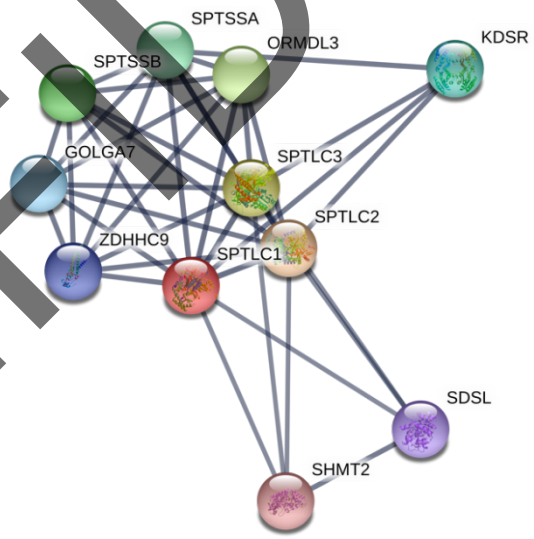

Figure 10 - STRING functional protein network prediction for SPTLC1 with confidence network edges.

Node 1	Node 2	Experimentally determined interaction	Co-expression	Phylogenetic Co-occurrence	Database score	Combined score
SPTLC1	SPTLC2	0.827	0.266	0.439	0.9	0.987
SPTLC3	SPTLC1	0.813	0.266	0.441	0.9	0.986
ORMDL3	SPTLC1	0.582	0.144	0	0.9	0.961
SPTSSB	SPTLC2	0.328	0.061	0	0.9	0.931
SPTLC3	SPTSSB	0.328	0.061	0	0.9	0.931
SPTSSB	SPTLC1	0.328	0	0	0.9	0.929
SPTSSA	SPTLC1	0.328	0	0	0.9	0.929
SPTSSA	SPTLC2	0.328	0	0	0.9	0.929
SPTLC3	SPTSSA	0.328	0	0	0.9	0.929
SPTLC3	ORMDL3	0.195	0.084	0	0.9	0.919

Table 1 - Top 10 highest-confidence relationships in STRING network.

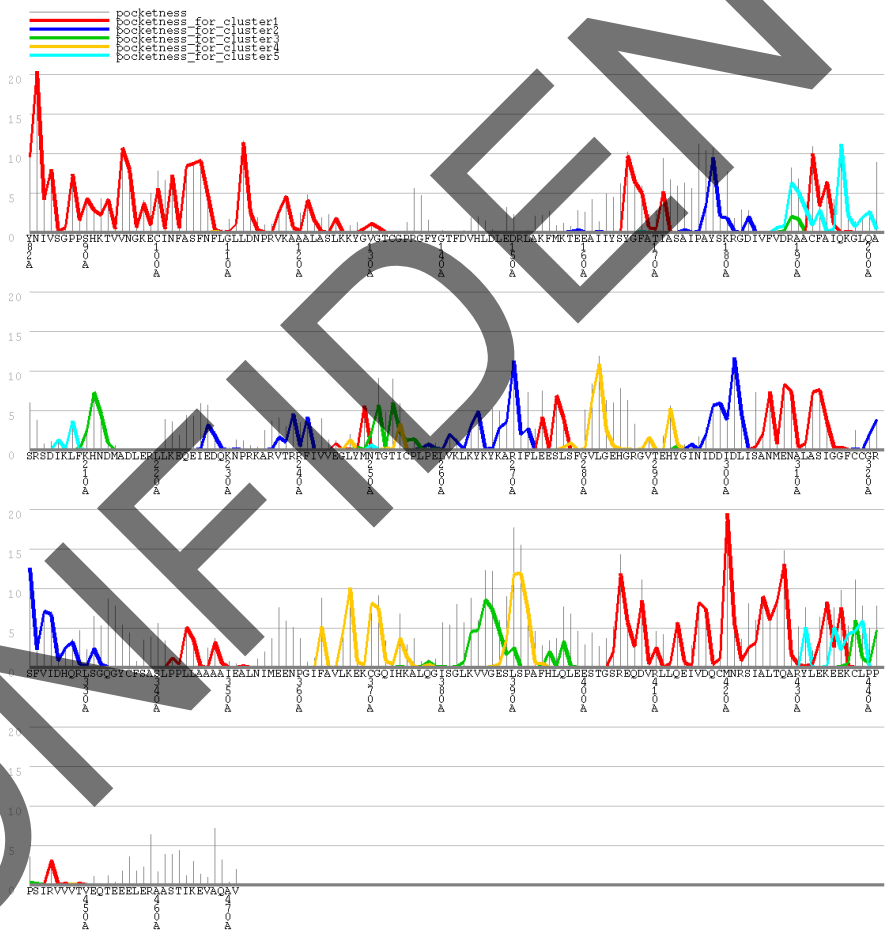

Figure 11 - SPTLC1 GHECOM residue-based pocketness predictions, for a maximum radius for large probe of 10 Å. Pocketness [%] is reported on the y-axis, indicating the size and depth of the pocket at a certain residue. 100% is related to the maximum depth accessible by the whole shell used by the morphological mathematic GHECOM algorithm.

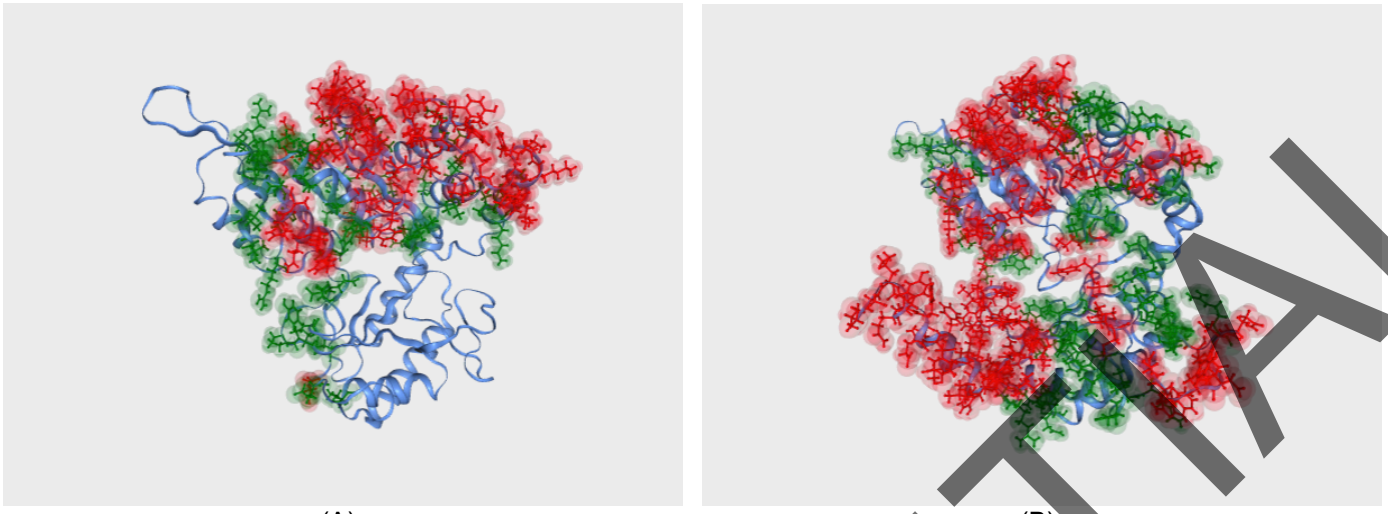

(A) (B)

Figure 12 - CPORT predicted active (green) and passive (red) residues for SPTLC1 (A) and SPTLC2 (B).

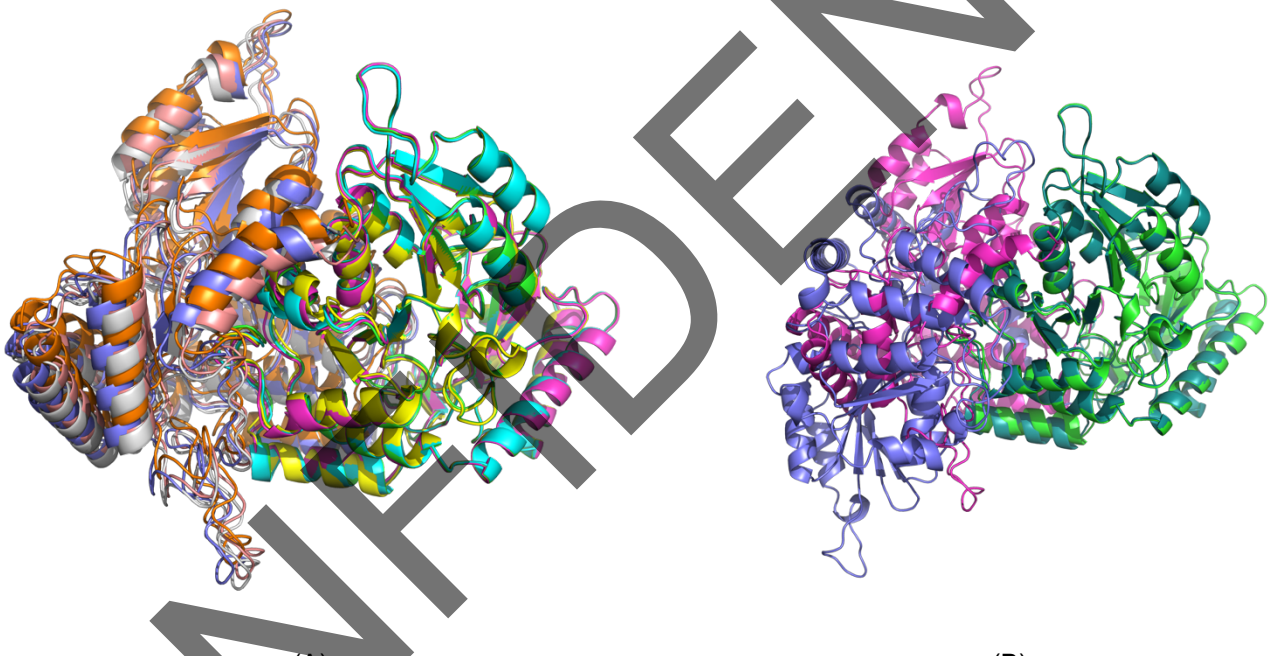

(A) (B)

Figure 13 - HADDOCK docking predictions PyMOL visualizations for SPTLC1 and SPTLC2 interaction. (A) Alignment on SPTLC1^{WT} of the 4 best structures of the cluster with the best HADDOCK-score. Both SPTLC1 and SPTLC2 enzymes are displayed. In decreasing order of HADDOCK score: SPTLC1^{WT} = {Green; Cyan; Magenta; Yellow}; SPTLC2^{WT}: {Salmon Pink; Gray; Purple; Orange} (B) SPTLC1 alignment of the best HADDOCK prediction for SPTLC1^{WT} and W SPTLC1^{C133W}. Light Green: SPTLC1^{WT}; Deep Green: SPTLC1^{C133W}; Magenta: SPTLC2^{WT} docked on SPTLC1^{WT}; Purple: SPTLC2^{WT} docked on SPTLC1^{C133W}.

SPTLC1 (WT / C133W)		Common binding residues for *SPTLC1*$^{C133W/WT}$	Central Cluster Residue	Binding Sites Clusters	*GHECOM* Clusters	SPTLC2 (WT)	
Res. Nb.	Res. Name					Res. Nb.	Res. Name
86	SER	-	-	-	1	199	TYR
112	LEU	-	-	-	1	114	LEU
118	LYS		A	A [+0]	1	112	VAL
118	LYS		A	A [+0]	1	113	SER
118	LYS		A	A [+0]	1	196	LEU
118	LYS		A	A [+0]	1	197	GLU
125	LEU	-	-	B [-1]	1	271	ARG
127	LYS		B	B [+0]	-	141	VAL
127	LYS		B	B [+0]	-	271	ARG
131	GLY	-	C	C [-2]	1	382	GLY
131	GLY	-	C	C [-2]	1	183	ARG
133	CYS	-	C	C [+0]	1	177	ASN
133	CYS	-	C	C [+0]	1	378	THR
138	PHE	-	-	C [-1]	-	136	ARG
139	TYR	-	D	D [+0]	-	265	SER
143	ASP	-	-	D [+4]	-	139	CYS
166	TYR	-	-	-	1	409	THR
201	ALA	-	-	-	5	159	SER
203	ARG	-	-	-	-	153	SER
301	ASP	-	-	-	2	115	TYR
308	GLU	-	E	E [+0]	1	204	CYS
313	SER	-	-	E [+5]	1	115	TYR
323	PHE	-	-	F [-4]	2	201	ALA
327	HIS		F	F [+0]	2	119	GLU
327	HIS		F	F [+0]	2	200	GLY
339	ALA		G	G [+0]	-	134	TRP
339	ALA		G	G [+0]	-	237	MET
434	LYS	-	H	H [+0]	1 5	209	GLU
435	GLU	-	-	H [+1]	1 5	407	TYR

Table 2 - Polar contacts (H-bonds) between docked SPTLC1 and SPTLC2. The central residue is the one selected as binding site center for virtual screening. The binding site radius is set to 10 Å; clusters include the potentially included residues within the binding site spherical space. Green: common H-bonds for SPTLC1^{WT} *and SPTLC1*^{C133W}*; Yellow: H-bonds uniquely present for SPTLC1*^{WT}*; Orange: H-bonds uniquely present for SPTLC1*^{C133W}*.*

Property name	Minimal value	Maximal value	Weight in final score	Justification
Molecular weight	180	480	0.8	Min and Max according to the Ghose filter. LRO5 indicates MW <= 500 but no lower bound. Selected weight is 0.8 because this is a very common rule but we leave a little bit of flexibility to explore a greater chemical space and find non-standard drugs. The weight also allows not to be very strict on the chosen compromise between the different rules.
Number of atoms (H excluded)	10	70	0.4	Ghose filter. Less common filter, therefore chose half of very common filter weight.
Number of H-donors	0	4	0.8	Compromise between LRO5 (<= 5) and RO3 (<= 3). Selected weight is 0.8 because this is a very common rule, but we leave a little bit of flexibility to explore a greater chemical space and find non-standard drugs. The weight also allows not to be very strict on the chosen compromise between the different rules.
Number of H-acceptors	0	8	0.8	Compromise between LRO5 (<=10) and RO3 (<=3). Selected weight is 0.8 because this is a very common rule, but we leave a little bit of flexibility to explore a greater chemical space and find non-standard drugs. The weight also allows not to be very strict on the chosen compromise between the different rules.
Polar solvent accessible surface area	0	140	0.4	Veber's rule. Less common filter, therefore chose half of very common filter weight.
Fraction of sp3-hybridized C	-	-	0	Not very common
Volume	-	-	0	Not very common
Area	-	-	0	Not very common
Number of rotatable bonds	0	8	0.4	Compromise between Veber's rule (<=10), R=3 (<=3), Lepre et al. (2<=N<=8). Less common filter, therefore chose half of very common filter weight. The weight also allows not to be very strict on the chosen compromise between the different rules.
Number of rings	1	6	0.2	Lepre et al. (1<=N<=6). Less common filter.
Number of aromatic rings	0	3	0	Lepre et al. (<=3). Less common filter, consider only number of rings.

Table 3 - Molecular properties and respective weights selected for the computation of the in-silico screening LEA3D genetic algorithm fitness score computation.

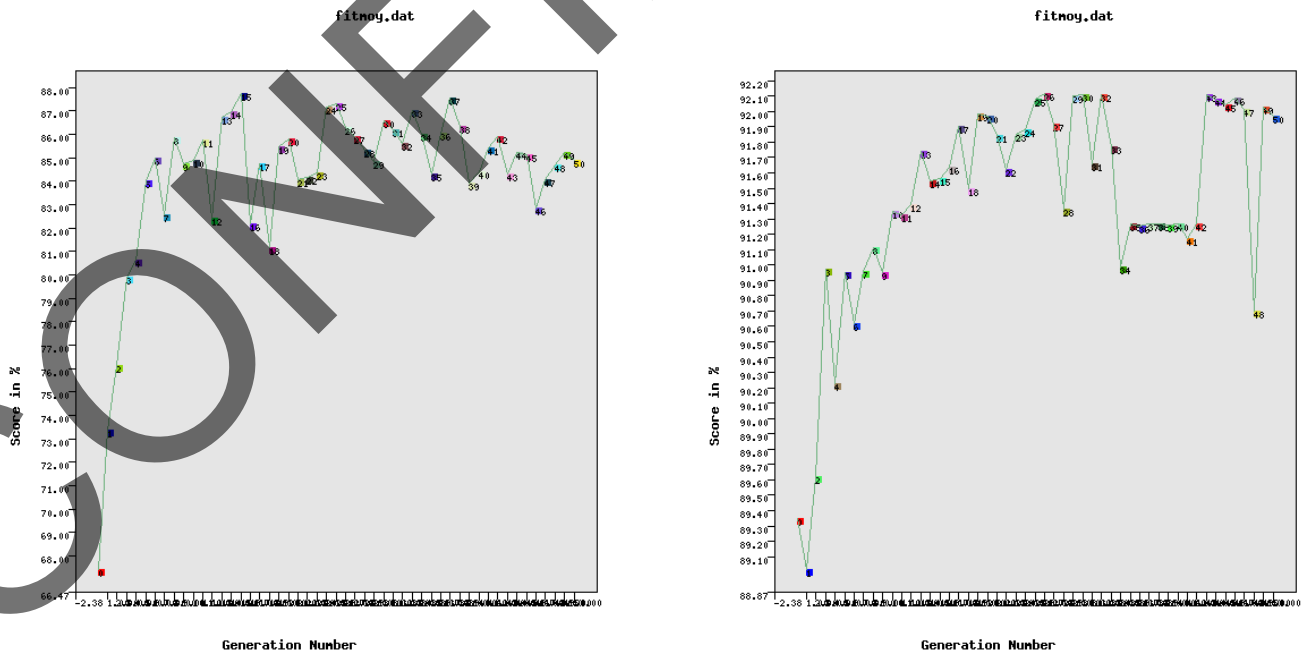

(A) (B)

Figure 14 - Example of LEA3D score evolution over generations of the genetic algorithm for the 139TYR simulation. (A) Generations mean score; (B) Best solution score for each generation.

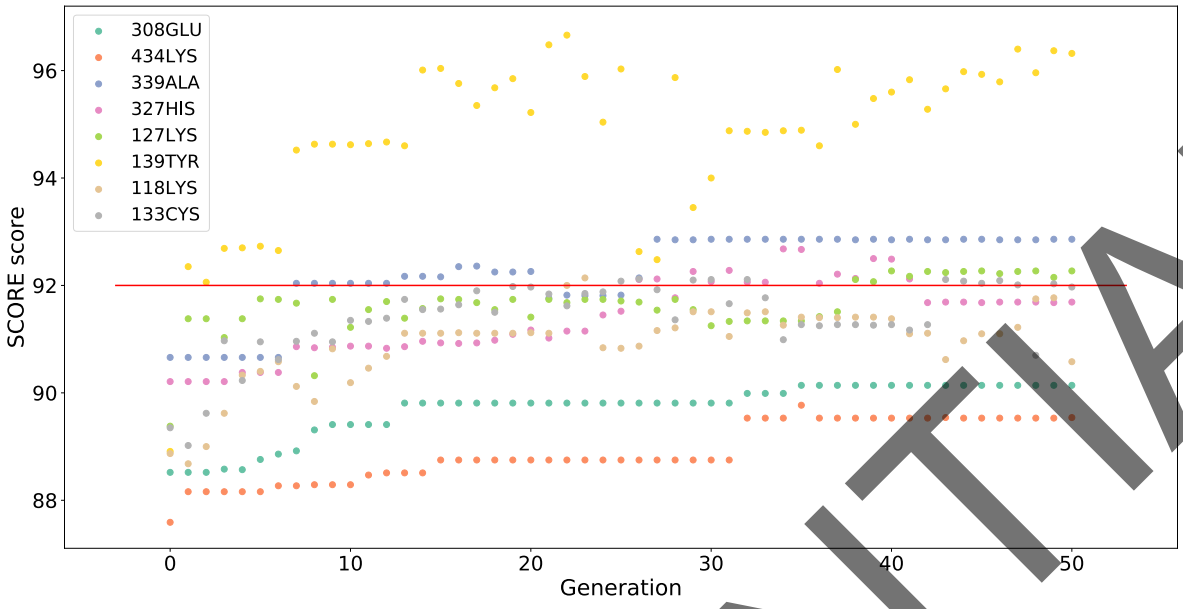

Figure 15 - Output of the simulations and thresholding example. Each point corresponds to a molecule resulting from LEA3D simulations; each color corresponds to a simulation for a given target binding site on SPTLC1^{WT}. The red line indicates a threshold of 92% used for the selection of the library.

Target selection table

The following table summarizes the initial research work that was carried out by our company. To identify a suitable target in the ceramide pathway, an in-depth literature study was performed for all involved enzymes. For each of them, the presence of a protein structure, the associated known diseases, the tissue specificity of the expression, the cellular location, the existence of ongoing clinical or in vitro trials related to the enzymatic target, and the results of other studies such as GWAs were assessed. This allowed us to select the most suitable enzyme (SPT) as our innovative drug target.

Table 4 - Target selection table

Enzyme	Full enzyme name	Reaction	Genes	Tissue specificity	Cellular location	Mendelian diseases
SPT	serine-palmitoyl transferase	Serine + palmitoyl-CoA -> 3-Ketosphinganine	SPTLC1-SPTLC2	Not tissue specific	ER	HSNP Type 1
3-ketosphinganine reductase		3-Ketosphinganine -> Sphinganine	TSC10		ER	None
CerS-1	ceramide synthase 1	Sphinganine + C18 -> dihydroceramide	CERS1 chr9	Brain, skeletal muscle, testis	ER	None
CerS-2	ceramide synthase 2	Sphinganine + C20/22/24/26 -> dihydroceramide	CERS2	Kidney, liver (and low levels in others)	ER	None
CerS-3	ceramide synthase 3	Sphinganine + C22/24/26 -> dihydroceramide	CERS3	Testis, skin	ER	None
CerS-4	ceramide synthase 4	Sphinganine + C18/20 -> dihydroceramide	CERS4	Low expression levels in all tissues, more in skin, leukocytes, heart, liver	ER	None
CerS-5	ceramide synthase 5	Sphinganine + C16 -> dihydroceramide	CERS5	Low expression levels in all tissues	ER	None
CerS-6	ceramide synthase 6	Sphinganine + C14/16 -> dihydroceramide	CERS6	Low expression levels in all tissues	ER	None
DES	Dihydroceramide desaturase	Dihydroceramide -> Ceramide			ER	None
SMase4	Sphingomyelin phosphodiesterase 4	Sphingomyelin ->Ceramide	SMPD4	Low tissue specificity, detected in all tissues	mainly nuclear membrane and additionally in cytosol	Niemann-Pick Type 3
SMase3	Sphingomyelin phosphodiesterase 3		SMPD3	Detected in all tissues Most abundant in gastrointestinal tract	ER	None
SMase2	Sphingomyelin phosphodiesterase 2		SMPD2	Low tissue specificity, detected in all tissues	Main location is vesicles and plasma membrane Additional location at cell junctions	None
SMase1	Sphingomyelin phosphodiesterase 1 (SPMD1)/Acid sphingomyelinase (ASM)		SMPD1 chr.11	Low tissue specificity, detected in all tissues	lysosome, secreted	Niemann-Pick disease A, B (AR)
CERT	Ceramide transfer protein	Transport from ER to Golgi	CERT chr.5	widely expressed : fat, thyroid	Cytoplasm, Golgi apparatus, ER	Mental retardation MRD34
CERK	Ceramide kinase	Ceramide -> Ceramide1P	CERK chr. 22	Low tissue/cell line specificity	Only in vesicles	None

Enzyme	Full enzyme name	Reaction	Genes	Tissue specificity	Cellular location	Mendelian diseases
SGMS1	Sphingomyelin synthase	Ceramide + Phosphatidylcholine -> Sphingomyelin + DAG and reverse reaction	SGMS2 chr. 10	Low tissue specificity, detected in all tissues, more so in skin cells	Nucleoplasm, Golgi, cytosol	None
SGMS2	Sphingomyelin synthase	Ceramide + Phosphatidylcholine -> Sphingomyelin + DAG and reverse reaction	SGMS2 chr. 4	Low tissue specificity, detected in all tissues except skin cells	Golgi, plasma membrane	None
CDase	Ceramidase	Ceramide -> Sphingosine	ACER 1 ACER 2 ACER 3 ASAH 1		nCDase: ER, aCDase: lysosome	Farber disease
SGPP	Sphingosine1P phosphatase	Sphingosine1P -> Sphingosine	SGPP1 SGPP2	Not specific, highest in placenta and kidney	ER, Plasma membrane	None
CerS-1	ceramide synthase 1	Sphingosine -> Ceramide	CERS1 chr9	Not tissue specific (high in globus pallidus)	ER	Epilepsy EPM8
CerS-2	ceramide synthase 2	Sphingosine -> Ceramide	CERS2	kidney, liver, brain, heart, placenta and lung	ER	None
CerS-3	ceramide synthase 3	Sphingosine -> Ceramide	CERS3	Epidermis	ER	Ichthyosis ARCI9
CerS-4	ceramide synthase 4	Sphingosine -> Ceramide	CERS4	Not tissue specific	ER	None
CerS-5	ceramide synthase 5	Sphingosine -> Ceramide	CERS5	Not tissue specific (high in cerebellum)	ER	None
CerS-6	ceramide synthase 6	Sphingosine -> Ceramide	CERS6	Adipose tissues (upregulated when obese)	ER	None
SPHK1	Sphingosine kinase 1	Sphingosine -> Sphingosine1P	SPHK1	Not tissue specific	Plasma membrane, cytoplasm	None
SPHK2	Sphingosine kinase 2	Sphingosine -> Sphingosine1P	SPHK2	Not tissue specific	Vesicles	None
S1P lyase	Sphingosine1P lyase	Sphingosine1P -> Ehanolamine1P + C16 fatty aldehyde	SGPL1	Not tissue specific	ER	None
GCDase	Galactosyl ceramidase	Galactosylceramide -> Ceramide	GALC	Testis, brain, placenta, kidney, liver	Lysosome	Krabble disease
GlcCDase	Glucosyl ceramidase	Glucosylceramide -> Ceramide	GBA	Not specific, highest in blood	Lysosome	Gaucher disease
	non-lysosomal glucosyl ceramidase	Glucosylceramide -> Ceramide	GBA2		ER, Golgi	None

Fluorescence polarization dye choice

An appropriate dye is chosen depending on the needs. The most important property is the fluorescence lifetime, where long lifetimes are desirable for larger proteins. In our application we are interested in a change in molecular weight between 53 KDa (*SPTLC1*) and 116 KDa (*SPTLC1-SPTLC2* dimer). Dansyl dyes would be best suited, with a fluorescence lifetime of around 20 ns.

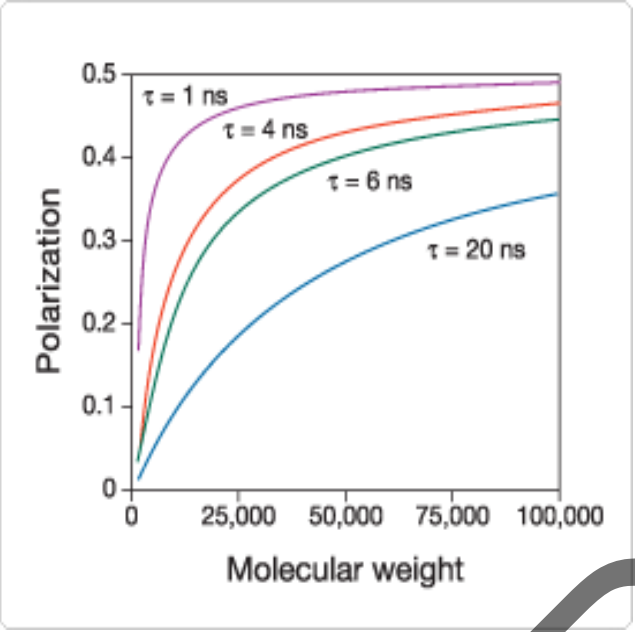

Figure 16 - Polarization curves for different fluorescence lifetimes[104]. Cyanine dyes in purple, fluorescein in red, BODIPY dyes in green and dansyl dyes in blue.

Bibliography

[1] Stith, J. L., Velazquez, F. N., & Obeid, L. M. (2019). Advances in determining signaling mechanisms of ceramide and role in disease. *Journal of lipid research*, *60*(5), 913-918.

[2] Hannun, Y. A., & Obeid, L. M. (2011). Many ceramides. *Journal of Biological Chemistry*, *286*(32), 27855-27862.

[3] Czubowicz, K., Jęśko, H., Wencel, P., Lukiw, W. J., & Strosznajder, R. P. (2019). The role of ceramide and sphingosine-1-phosphate in Alzheimer's disease and other neurodegenerative disorders. *Molecular neurobiology*, 1-20.

[4] Hannun, Y. A., & Obeid, L. M. (2018). Sphingolipids and their metabolism in physiology and disease. *Nature reviews Molecular cell biology*, *19*(3), 1§75.

[5] Vanier, M. T. (2010). Niemann-Pick disease type C. *Orphanet journal of rare diseases*, *5*(1), 16.

[6] Auer-Grumbach, M. (2008). Hereditary sensory neuropathy type I. *Orphanet journal of rare diseases*, *3*(1), 7.

[7] "Hereditary sensory neuropathy type IA - Genetics Home ...." 12 nov.. 2019, https://ghr.nlm.nih.gov/condition/hereditary-sensory-neuropathy-type-ia. Date de consultation : 24 nov.. 2019.

[8] "Hereditary Sensory Neuropathy Type I - NORD (National ...." https://rarediseases.org/rare-diseases/hereditary-sensory-neuropathy-type-i/. Date de consultation : 24 nov.. 2019.

[9] "Hereditary Sensory and Autonomic Neuropathy Type II ...." https://rarediseases.org/rare-diseases/hereditary-sensory-and-autonomic-neuropathy-type-ii/. Date de consultation : 24 nov.. 2019.

[10] "Hereditary Sensory and Autonomic Neuropathy Type IV ...." https://rarediseases.org/rare-diseases/hereditary-sensory-and-autonomic-neuropathy-type-iv/. Date de consultation : 24 nov.. 2019.

[11] Bode, H., Bourquin, F., Suriyanarayanan, S., Wei, Y., Alecu, I., Othman, A., ... & Hornemann, T. (2015). HSAN1 mutations in serine palmitoyltransferase reveal a close structure–function–phenotype relationship. *Human molecular genetics*, *25*(5), 853-865.

[12] Gantner, M. L., Eade, K., Wallace, M., Handzlik, M. K., Fallon, R., Trombley, J., ... & Sauer, L. (2019). Serine and lipid metabolism in macular disease and peripheral neuropathy. *New England Journal of Medicine*, *381*(15), 1422-1433.

[13] Schachat, A. P., Wilkinson, C. P., Hinton, D. R., Wiedemann, P., Freund, K. B., & Sarraf, D. (2017). *Ryan's Retina E-Book*. Elsevier Health Sciences.

[14] Issa, P. C., Gillies, M. C., Chew, E. Y., Bird, A. C., Heeren, T. F., Peto, T., ... & Scholl, H. P. (2013). Macular telangiectasia type 2. *Progress in retinal and eye research*, *34*, 49-77.

[15] Hornemann, T., Richard, S., Rütti, M. F., Wei, Y., & von Eckardstein, A. (2006). Cloning and initial characterization of a new subunit for mammalian serine-palmitoyltransferase. Journal of Biological Chemistry, 281(49), 37275-37281.

[16] Szklarczyk, D., Gable, A. L., Lyon, D., Junge, A., Wyder, S., Huerta-Cepas, J., ... & Jensen, L. J. (2018). STRING v11: protein–protein association networks with increased coverage, supporting functional discovery in genome-wide experimental datasets. Nucleic acids research, 47(D1), D607-D613.

[17] Davis, D., Kannan, M., & Wattenberg, B. (2018). Orm/ORMDL proteins: Gate guardians and master regulators. Advances in biological regulation, 70, 3-18.

[18] Gupta, S. D., Gable, K., Alexaki, A., Chandris, P., Proia, R. L., Dunn, T. M., & Harmon, J. M. (2015). Expression of the ORMDLS, modulators of serine palmitoyltransferase, is regulated by sphingolipids in mammalian cells. Journal of Biological Chemistry, 290(1), 90-98.

[19] Bienert, S., Waterhouse, A., de Beer, T. A., Tauriello, G., Studer, G., Bordoli, L., & Schwede, T. (2016). The SWISS-MODEL Repository—new features and functionality. Nucleic acids research, 45(D1), D313-D319.

[20] Van Zundert, G. C. P., Rodrigues, J. P. G. L. M., Trellet, M., Schmitz, C., Kastritis, P. L., Karaca, E., ... & Bonvin, A. M. J. J. (2016). The HADDOCK2. 2 web server: user-friendly integrative modeling of biomolecular complexes. Journal of molecular biology, 428(4), 720-725.

[21] de Vries, S. J., & Bonvin, A. M. (2011). CPORT: a consensus interface predictor and its performance in prediction-driven docking with HADDOCK. PloS one, 6(3), e17695.

[22] Kawabata, T. (2010). Detection of multiscale pockets on protein surfaces using mathematical morphology. Proteins: Structure, Function, and Bioinformatics, 78(5), 1195-1211

[23] Douguet, D., Munier-Lehmann, H., Labesse, G., & Pochet, S. (2005). LEA3D: a computer-aided ligand design for structure-based drug design. Journal of medicinal chemistry, 48(7), 2457-2468.

[24] Lipinski, C. A. (2004). Lead-and drug-like compounds: the rule-of-five revolution. Drug Discovery Today: Technologies, 1(4), 337-341.

[25] Barker, J., Hesterkamp, T., & Whittaker, M. (2008). Integrating HTS and fragment-based drug discovery. DDW DRUG DISCOVERY WORLD, 9(3), 69.

[26] Guvench, O. (2016). Computational functional group mapping for drug discovery. Drug discovery today, 21(12), 1928-1931.

[27] Guvench, O., & MacKerell Jr, A. D. (2009). Computational fragment-based binding site identification by ligand competitive saturation. PLoS computational biology, 5(7), e1000435.

[28] Segler, M. H., Preuss, M., & Waller, M. P. (2018). Planning chemical syntheses with deep neural networks and symbolic AI. Nature, 555(7698), 604.

[29] "Biomolecular Screening Facility BSF - EPFL." 29 oct.. 2018, https://bsf.epfl.ch/. Date de consultation : 29 nov.. 2019.

[30] Vedani, A., Dobler, M., Hu, Z., & Smieško, M. (2015). OpenVirtualToxLab—a platform for generating and exchanging in silico toxicity data. Toxicology letters, 232(2), 519-532.

[31] Pires, D. E., Blundell, T. L., & Ascher, D. B. (2015). pkCSM: predicting small-molecule pharmacokinetic and toxicity properties using graph-based signatures. Journal of medicinal chemistry, 58(9), 4066-4072.

[32] Gao, J., Ellis, L. B., & Wackett, L. P. (2009). The University of Minnesota biocatalysis/biodegradation database: improving public access. Nucleic acids research, 38(suppl_1), D488-D491.

[33] Liao, C., Sitzmann, M., Pugliese, A., & Nicklaus, M. C. (2011). Software and resources for computational medicinal chemistry. Future medicinal chemistry, 3(8), 1057-1085.

[34] "Switzerland (Schweiz) | Sigma-Aldrich." https://www.sigmaaldrich.com/switzerland-schweiz.html. Date de consultation : 15 nov.. 2019.

[35] "Karebay: Peptide Synthesis, Gene Synthesis, Antibody ...." https://www.karebaybio.com/. Date de consultation : 15 nov.. 2019.

[36] Hojjati, M. R., Li, Z., & Jiang, X. C. (2005). Serine palmitoyl-CoA transferase (SPT) deficiency and sphingolipid levels in mice. *Biochimica et Biophysica Acta (BBA)-Molecular and Cell Biology of Lipids*, *1737*(1), 44-51.

[37] Wadsworth, J. M., Clarke, D. J., McMahon, S. A., Lowther, J. P., Beattie, A. E., Langridge-Smith, P. R., ... & Campopiano, D. J. (2013). The chemical basis of serine palmitoyltransferase inhibition by myriocin. *Journal of the American Chemical Society*, *135*(38), 14276-14285.

[38]Larsson, J. (2009). Methods for measurement of solubility and dissolution rate of sparingly soluble drugs.

[39] Du, Yuhong. "Fluorescence polarization assay to quantify protein-protein interactions in an HTS format." *Protein-Protein Interactions*. Humana Press, New York, NY, 2015. 529-544.

[40] Azad, Taha, Amin Tashakor, and Saman Hosseinkhani. "Split-luciferase complementary assay: applications, recent developments, and future perspectives." *Analytical and bioanalytical chemistry* 406.23 (2014): 5541-5560.

[41] Kasumov, T., Huang, H., Chung, Y. M., Zhang, R., McCullough, A. J., & Kirwan, J. P. (2010). Quantification of ceramide species in biological samples by liquid chromatography electrospray ionization tandem mass spectrometry. *Analytical biochemistry*, *401*(1), 154-161.

[42] Segall, M. D., & Barber, C. (2014). Addressing toxicity risk when designing and selecting compounds in early drug discovery. *Drug discovery today*, *19*(5), 688-693.

[43] Tolosa, L., Donato, M. T., & Gómez-Lechón, M. J. (2015). General cytotoxicity assessment by means of the MTT assay. In *Protocols in In Vitro Hepatocyte Research* (pp. 333-348). Humana Press, New York, NY..

[44] Suzen, S., Gurer-Orhan, H., & Saso, L. (2017). Detection of reactive oxygen and nitrogen species by electron paramagnetic resonance (EPR) technique. *Molecules*, *22*(1), 181.

[45] Whitebread, S., Dumotier, B., Armstrong, D., Fekete, A., Chen, S., Hartmann, A., ... & Urban, L. (2016). Secondary pharmacology: screening and interpretation of off-target activities–focus on translation. *Drug discovery today*, *21*(8), 1232-1242.

[46] Deaton, A. M., Fan, F., Zhang, W., Nguyen, P. A., Ward, L. D., & Nioi, P. (2018). Rationalizing secondary pharmacology screening using human genetic and pharmacological evidence. *Toxicological Sciences*, *167*(2), 593-603.

[47] Keserű, G. M., & Makara, G. M. (2006). Hit discovery and hit-to-lead approaches. *Drug discovery today*, *11*(15-16), 741-748.

[48] Hubbard, R. E. (2008). Fragment approaches in structure-based drug discovery. *Journal of synchrotron radiation*, *15*(3), 227-230.
[49] van Breemen, R. B., & Li, Y. (2005). Caco-2 cell permeability assays to measure drug absorption. *Expert opinion on drug metabolism & toxicology*, *1*(2), 175-185.
[50] Lodish, H., Berk, A., Zipursky, S. L., Matsudaira, P., Baltimore, D., & Darnell, J. (2000). Molecular cell biology 4th edition. Section 8.1 Mutations : Types and causes. *National Center for Biotechnology Information, Bookshelf*.
[51] Tejs, S. (2008). The Ames test: a methodological short review. *Environmental Biotechnology*, *4*, 7-14.
[52] Kulis-Horn, R. K., Persicke, M., & Kalinowski, J. (2014). Histidine biosynthesis, its regulation and biotechnological application in Corynebacterium glutamicum. *Microbial biotechnology*, *7*(1), 5-25.
[53] Proudlock, R. (Ed.). (2016). *Genetic Toxicology Testing: A Laboratory Manual. Chapter 6 - The In Vitro Micronucleus Assay*. Academic Press.
[54] Gao, S., & Lai, L. (2018). Synthetic lethality in drug development: the dawn is coming.
[55] Birkebak, J., Buckley, L. A., Dambach, D., Musvasva, E., Price, K., Ralston, S., & Sacaan, A. (2019). Pharmaceutical industry perspective on combination toxicity studies: Results from an intra-industry survey conducted by IQ DruSafe Leadership Group. *Regulatory Toxicology and Pharmacology*, *102*, 40-46.
[56] "Guideline on Fixed Combinations - European Medicines Agency." 24 janv.. 2008, https://www.ema.europa.eu/documents/scientific-guideline/guideline-non-clinical-development-fixed-combinations-medicinal-products_en.pdf. Date de consultation : 24 nov.. 2019.
[57] "Download the Final Guidance Document - FDA." https://www.fda.gov/media/119657/download. Date de consultation : 24 nov.. 2019.
[58] Kar, S., & Leszczynski, J. (2019). Exploration of computational approaches to predict the toxicity of chemical mixtures. *Toxics*, *7*(1), 15.
[59] Seiler, A. E., & Spielmann, H. (2011). The validated embryonic stem cell test to predict embryotoxicity in vitro. *Nature protocols*, *6*(7), 961.
[60] Fonsi, M., Orsale, M. V., & Monteagudo, E. (2008). High-throughput microsomal stability assay for screening new chemical entities in drug discovery. *Journal of biomolecular screening*, *13*(9), 862-869.
[61] Iwatsubo, T., Hirota, N., Ooie, T., Suzuki, H., Shimada, N., Chiba, K., ... & Sugiyama, Y. (1997). Prediction of in vivo drug metabolism in the human liver from in vitro metabolism data. *Pharmacology & therapeutics*, *73*(2), 147-171.
[62] Fligor, C. M., Langer, K. B., Sridhar, A., Ren, Y., Shields, P. K., Edler, M. C., ... & Suter, D. M. (2018). Three-dimensional retinal organoids facilitate the investigation of retinal ganglion cell development, organization and neurite outgrowth from human pluripotent stem cells. *Scientific reports*, *8*(1), 14520.
[63] "Good laboratory practice compliance | European Medicines ...." https://www.ema.europa.eu/en/human-regulatory/research-development/compliance/good-laboratory-practice-compliance. Accessed 25 Nov. 2019.
[64] McAnally, D., Vicchiarelli, M., Siddiquee, K., & Smith, L. H. (2012). In vivo rapid assessment of compound exposure (RACE) for profiling the pharmacokinetics of novel chemical probes. *Current protocols in chemical biology*, *4*(4), 299-309.
[65]Chung, T. D., Terry, D. B., & Smith, L. H. (2015). In vitro and in vivo assessment of ADME and PK properties during lead selection and lead optimization–guidelines, benchmarks and rules of thumb. In *Assay Guidance Manual [Internet]*. Eli Lilly & Company and the National Center for Advancing Translational Sciences.
[66] Fan, J. (2014). De Lannoy IaM. *Pharmacokinetics. Biochem. Pharmacol*, *87*(1), 93-120.
[67] Sleigh, J. N., Weir, G. A., & Schiavo, G. (2016). A simple, step-by-step dissection protocol for the rapid isolation of mouse dorsal root ganglia. *BMC research notes*, *9*(1), 82.
[68] Zhang, D., Luo, G., Ding, X., & Lu, C. (2012). Preclinical experimental models of drug metabolism and disposition in drug discovery and development. *Acta Pharmaceutica Sinica B*, *2*(6), 549-561.
[69] Zhang, Z., & Tang, W. (2018). Drug metabolism in drug discovery and development. *Acta Pharmaceutica Sinica B*, *8*(5), 721-732.
[70] "Safety Guidelines - ICH." https://www.ich.org/page/safety-guidelines. Date de consultation : 25 nov.. 2019.
[71] Fenech, M. (1993). The cytokinesis-block micronucleus technique: a detailed description of the method and its application to genotoxicity studies in human populations. *Mutation Research/Fundamental and Molecular Mechanisms of Mutagenesis*, *285*(1), 35-44.
[72] Mortelmans, K., & Zeiger, E. (2000). The Ames Salmonella/microsome mutagenicity assay. *Mutation research/fundamental and molecular mechanisms of mutagenesis*, *455*(1-2), 29-60.
[73] Gupta, P. K. (2016). Fundamentals of Toxicology: Essential Concepts and Applications. Academic Press.

[74] Garofalo, K., Penno, A., Schmidt, B. P., Lee, H. J., Frosch, M. P., von Eckardstein, A., ... & Eichler, F. S. (2011). Oral L-serine supplementation reduces production of neurotoxic deoxysphingolipids in mice and humans with hereditary sensory autonomic neuropathy type 1. *The Journal of clinical investigation*, *121*(12), 4735-4745.

[75] Aung, K. Z., Wickremasinghe, S. S., Makeyeva, G., Robman, L., & Guymer, R. H. (2010). The prevalence estimates of macular telangiectasia type 2: the Melbourne Collaborative Cohort Study. *Retina*, *30*(3), 473-478.

[76] McCampbell, A., Truong, D., Broom, D. C., Allchorne, A., Gable, K., Cutler, R. G., ... & Dunn, T. M. (2005). Mutant SPTLC1 dominantly inhibits serine palmitoyltransferase activity in vivo and confers an age-dependent neuropathy. *Human molecular genetics*, *14*(22), 3507-3521.

[77] Eichler, F. S., Hornemann, T., McCampbell, A., Kuljis, D., Penno, A., Vardeh, D., ... & Selig, M. (2009). Overexpression of the wild-type SPT1 subunit lowers desoxysphingolipid levels and rescues the phenotype of HSAN1. *Journal of Neuroscience*, *29*(46), 14646-14651.

[78] Triplett, J., Nicholson, G., Sue, C., Hornemann, T., & Yiannikas, C. (2019). Hereditary sensory and autonomic neuropathy type IC accompanied by upper motor neuron abnormalities and type II juxtafoveal retinal telangiectasias. *Journal of the Peripheral Nervous System*, *24*(2), 224-229.

[79] "Power and Sample Size." http://powerandsamplesize.com/. Date de consultation : 13 nov.. 2019.

[80] Othman, A., Saely, C. H., Muendlein, A., Vonbank, A., Drexel, H., von Eckardstein, A., & Hornemann, T. (2015). Plasma 1-deoxysphingolipids are predictive biomarkers for type 2 diabetes mellitus. *BMJ Open Diabetes Research and Care*, *3*(1), e000073.

[81] Smith, C. A., Hooper, M. L., & Chauhan, B. C. (2019). Optical Coherence Tomography Angiography in Mice: Quantitative Analysis After Experimental Models of Retinal Damage. *Investigative ophthalmology & visual science*, *60*(5), 1556-1565.

[82] Alert, O. (2005). Guidance for Industry Estimating the Maximum Safe Starting Dose in Initial Clinical Trials for Therapeutics in Adult Healthy Volunteers.

[83] Le Tourneau, C. *et al.* (2009). "Dose escalation methods in phase I cancer clinical trials." Journal of the National Cancer Institute vol. 101,10: 708-20. doi:10.1093/jnci/djp079

[84] Fridman, V. *et al.* (2019). "Randomized trial of l-serine in patients with hereditary sensory and autonomic neuropathy type 1." Neurology. Jan 22;92(4):e359-e370. doi: 10.1212/WNL.0000000000006811. Epub 2019 Jan 9.

[85] Kramer, R. *et al.* (2015). "Neurotoxic 1-deoxysphingolipids and paclitaxel-induced peripheral neuropathy." FASEB J. 10.1096/fj.15-272567.

[86] Tomohiro, K. *et al.* (2011). "Role of satellite cell-derived L-serine in the dorsal root ganglion in paclitaxel-induced painful peripheral neuropathy." Neuroscience. 174. 190-9. 10.1016/j.neuroscience.2010.11.046.

[87] Othman, A. *et al.* (2015). "Fenofibrate lowers atypical sphingolipids in plasma of dyslipidemic patients: a novel approach for treating diabetic neuropathy?" J. Clin. Lipidol., 9, pp. 568-575

[88] Bertea, M. *et al.* (2010). "Deoxysphingoid bases as plasma markers in Diabetes mellitus." *Lipids Health Dis* 9, 84 (2010) doi:10.1186/1476-511X-9-84

[89] Hannich, J.T. *et al.* (2019) "1-Deoxydihydroceramide causes anoxic death by impairing chaperonin-mediated protein folding." *Nat Metab* 1, 996–1008 doi:10.1038/s42255-019-0123-y

[90] Szklarczyk, D., Gable, A. L., Lyon, D., Junge, A., Wyder, S., Huerta-Cepas, J., ... & Jensen, L. J. (2018). STRING v11: protein–protein association networks with increased coverage, supporting functional discovery in genome-wide experimental datasets. Nucleic acids research, 47(D1), D607-D613.

[91] de Vries, S. J., & Bonvin, A. M. (2011). CPORT: a consensus interface predictor and its performance in prediction-driven docking with HADDOCK. PloS one, 6(3), e17695.

[92] Van Zundert, G. C. P., Rodrigues, J. P. G. L. M., Trellet, M., Schmitz, C., Kastritis, P. L., Karaca, E., ... & Bonvin, A. M. J. J. (2016). The HADDOCK2. 2 web server: user-friendly integrative modeling of biomolecular complexes. Journal of molecular biology, 428(4), 720-725.

[93] Schrödinger, L. The PyMOL Molecular Graphics System, version 1.8; Schrödinger, LLC, 2015.

[94] Laskowski, R. A., Hutchinson, E. G., Michie, A. D., Wallace, A. C., Jones, M. L., & Thornton, J. M. (1997). PDBsum: a Web-based database of summaries and analyses of all PDB structures. Trends in biochemical sciences, 22(12), 488-490.

[95] Ainavarapu, S. R. K., Brujić, J., Huang, H. H., Wiita, A. P., Lu, H., Li, L., ... & Fernandez, J. M. (2007). Contour length and refolding rate of a small protein

controlled by engineered disulfide bonds. Biophysical journal, 92(1), 225-233.
[96] Douguet, D., Munier-Lehmann, H., Labesse, G., & Pochet, S. (2005). LEA3D: a computer-aided ligand design for structure-based drug design. Journal of medicinal chemistry, 48(7), 2457-2468.
[97] Korb, O., Stützle, T., & Exner, T. E. (2006, September). PLANTS: Application of ant colony optimization to structure-based drug design. In International Workshop on Ant Colony Optimization and Swarm Intelligence (pp. 247-258). Springer, Berlin, Heidelberg.
[98] Lipinski, C. A. (2004). Lead-and drug-like compounds: the rule-of-five revolution. Drug Discovery Today: Technologies, 1(4), 337-341.
[99] Veber, D. F., Johnson, S. R., Cheng, H. Y., Smith, B. R., Ward, K. W., & Kopple, K. D. (2002). Molecular properties that influence the oral bioavailability of drug candidates. Journal of medicinal chemistry, 45(12), 2615-2623.
[100] Congreve, M., Carr, R., Murray, C., & Jhoti, H. (2003). A'rule of three'for fragment-based lead discovery?. Drug discovery today, 19(8), 876-877.
[101] Lepre, C. A. (2001). Library design for NMR-based screening. Drug Discovery Today, 6(3), 133-140.
[102] Xu, J., & Stevenson, J. (2000). Drug-like index: a new approach to measure drug-like compounds and their diversity. Journal of Chemical Information and Computer Sciences, 40(5), 1177-1187.
[103] O'Boyle, N. M., Banck, M., James, C. A., Morley, C., Vandermeersch, T., & Hutchison, G. R. (2011). Open Babel: An open chemical toolbox. Journal of cheminformatics, 3(1), 33.
[104] "Fluorescence Polarization (FP)—Note 1.4 | Thermo Fisher ...." https://www.thermofisher.com/us/en/home/references/molecular-probes-the-handbook/technical-notes-and-product-highlights/fluorescence-polarization-fp.html. Date de consultation : 26 nov.. 2019.